TEKST NR 378 2000

Solar energy preprints:

••

1. Renewable energy sources and thermal energy storage
2. Integration of photovoltaic cells into the global energy system

Bent Sørensen

ROSKILDE UNIVERSITY, INSTITUTE 2,
ENERGY & ENVIRONMENT GROUP

February 2000

TEKSTER fra

IMFUFA

RENEWABLE ENERGY SOURCES AND THERMAL ENERGY STORAGE INTEGRATION OF PHOTOVOLTAIC CELLS INTO THE GLOBAL ENERGY SYSTEM

Bent Sørensen (email bes@ruc.dk)

Abstract: The text contains two preprints, both of which deal with aspects of solar energy.

The first examines the heat energy storage options suitable for renewable energy sources and particularly those for solar thermal systems. It will be chapter 6 of a book on "Thermal energy storage systems and applications", edited by I. Dincer and planned for publication by Wiley, New York, by late 2000.

The second paper deals with the place of photovoltaic systems, for providing solar electricity in the future. It will appear as a chapter in "Renewable energy: trends and prospects", a book edited by S. Majumdar, E. Miller and A. Panah, planned for publication by The Pennsylvania Academy of Science, also by late 2000.

cover painting by the author.

TEKST NR 378 2000

Solar energy preprints:

1. Renewable energy sources and thermal energy storage
2. Integration of photovoltaic cells into the global energy system

Bent Sørensen

ROSKILDE UNIVERSITY, INSTITUTE 2,
ENERGY & ENVIRONMENT GROUP

February 2000

TEKSTER fra

IMFUFA

6

Renewable Energy Sources and Thermal Energy Storage

Bent Sørensen

6.1   Introduction

The use of renewable energy sources induces requirements for the associated energy systems, that are different from those pertaining to fossil energy systems. This is particularly the case for renewable energy source flows of an intermittent nature, such as direct solar radiation and wind energy, whereas a renewable energy source such as biomass more resembles fossil energy in its handling and storage requirements. Resources such as hydro are in between, with dependence on the nature of the water flow, e.g. river-based as opposed to lake- or reservoir-based. Matching renewable resource flows with demand profiles can be handled by using techniques of load shifting, of area shifting ("import-export"), of regulation-capable backup, or of energy storage. For systems aimed at thermal energy supply, thermal storage systems may be considered. For high-quality energy forms, only high-temperature thermal storage is relevant, due to thermodynamical conversion limitations.

   The technical options for energy storage are well described in the literature (see e.g. Jensen and Sørensen (1984) or Sørensen (2000)), and the treatment here will focus on system aspects. The emphasis will be on solar thermal energy use, where thermal storage is imperative. Biomass used for thermal or other energy purposes can be stored as a fuel and wind or solar electric energy will require storage forms other than thermal energy storage. Section 6.2 defines the problem to be looked into, by discussing the variations in solar radiation as function of time and geographical location, the variations in heat load again as function of time and place, and the requirements for thermal storage, that could enable it to complement the solar energy source flow to cover the demand continuously. Section 6.3 provides illustrative examples of actually installed equipment, and section 6.4 highlights the tools available for simulating the performance of concrete systems. In section 6.5, some longer-term perspectives will be presented, and section 6.6 gives some conclusions and impressions of the relative merits of different solutions to the supply-demand-matching problem.

6.2   Nature of the problem

The options for energy storage depend strongly on the length of storage required. The issue of technical stability on scales of seconds is usually not relevant for thermal systems, so the main distinction is between short-term storage dealing with the day-to-night or day-to day variations in solar radiation, and the long-term storage dealing with the seasonal variations in solar radiation, that occur at higher latitudes. Typical variations in solar radiation and heat demand are dealt with in the following subsections.

6.2.1   Solar radiation

Solar radiation data on horizontal planes are collected at many points at the surface of the Earth, and at some locations, primarily in cities, also data on inclined surface are measured. The standard meteorological equipment collects both direct and scattered radiation (or global and scattered radiation, from which the direct can be derived). More geographically uniform data can be derived from satellite measurements, based on models of absorption, reflection and attenuation processes within the atmosphere plus the balance requirements at the Earth's surface, combined with top of the atmosphere primary radiation data (Sørensen, 2000). One such set of data is shown in figures 6.1-6.2 (scale in Figure 6.5). These figures give the radiation on a horizontal plane at the Earth's surface for selected months of 1997 (NCEP/NCAR, 1998).
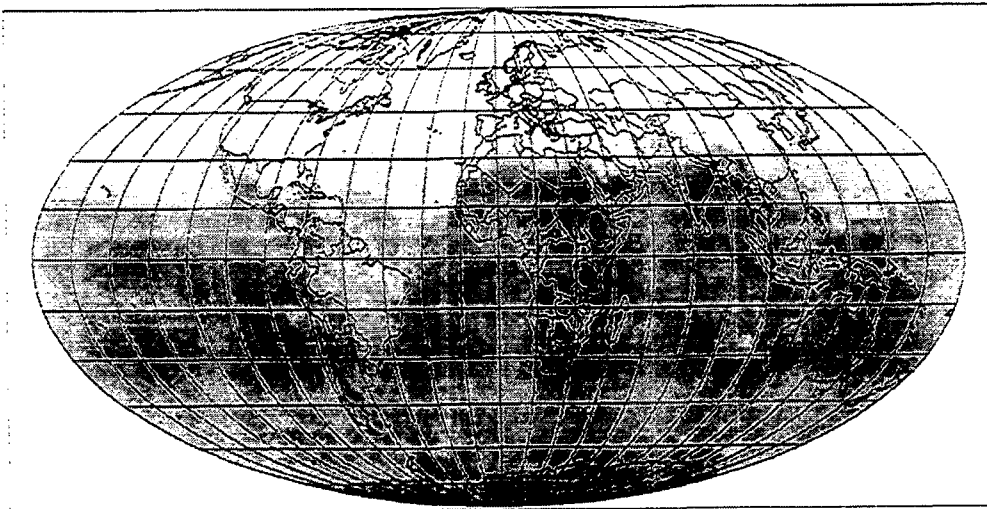

Figure 6.1 January 1997 average solar radiation on horizontal surface (downward energy flux at Earth's surface) (from Sørensen, 1999, based on data from NCEP/NCAR, 1998; scale given in Figure 6.5).

2

Figure 6.2 April 1997 average solar radiation on horizontal surface (downward energy flux at Earth's surface) (from Sørensen, 1999, based on data from NCEP/NCAR, 1998; scale given in Figure 6.5).
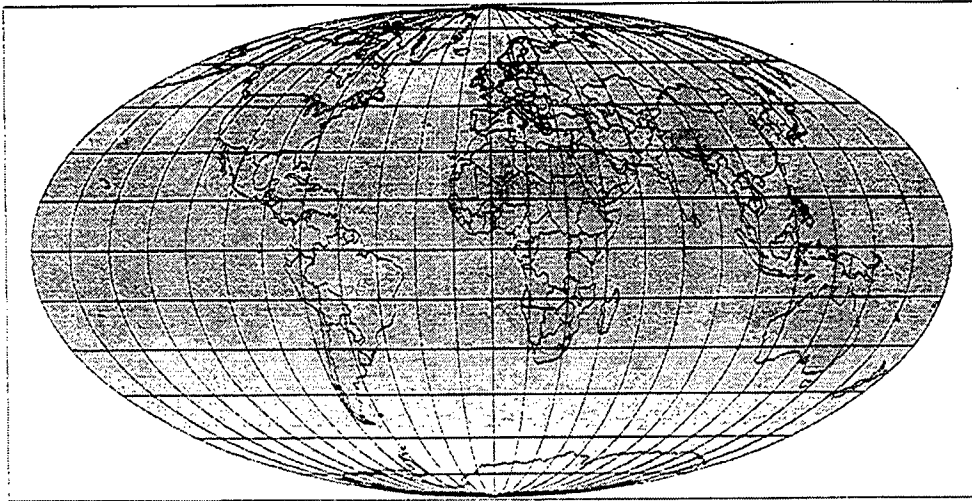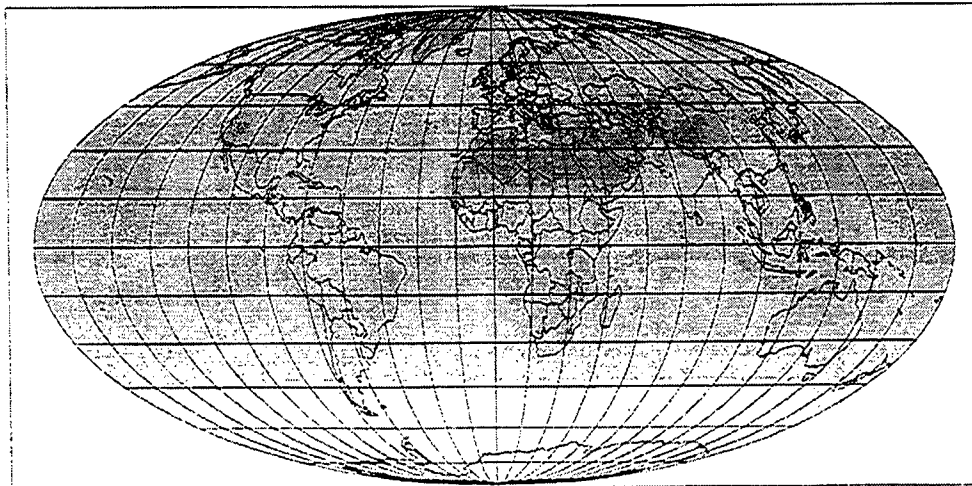

Figure 6.3 July 1997 average solar radiation on horizontal surface (downward energy flux at Earth's surface) (from Sørensen, 1999, based on data from NCEP/NCAR, 1998; scale given in Figure 6.5).

Figure 6.4 October 1997 average solar radiation on horizontal surface (downward energy flux at Earth's surface) (from Sørensen, 1999, based on data from NCEP/NCAR, 1998; scale given in Figure 6.5).
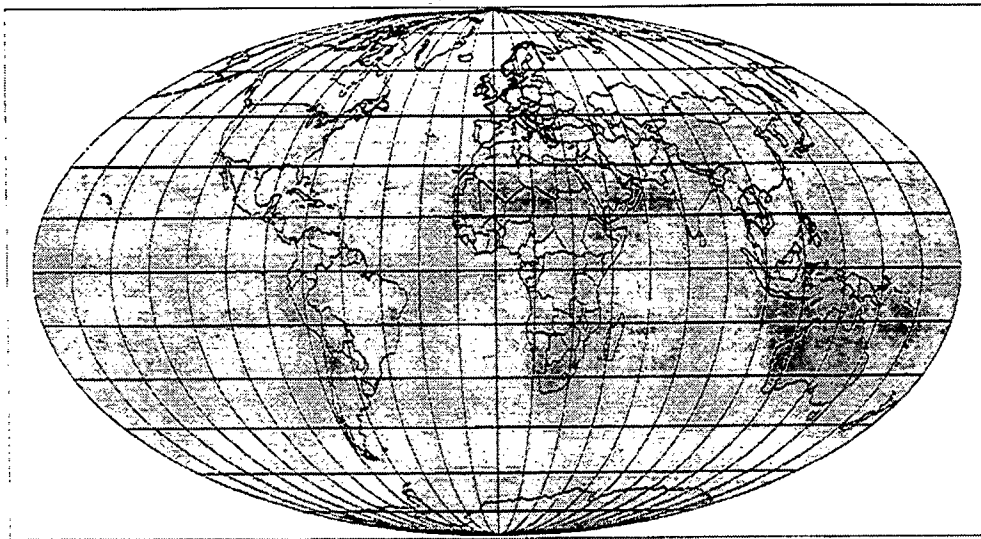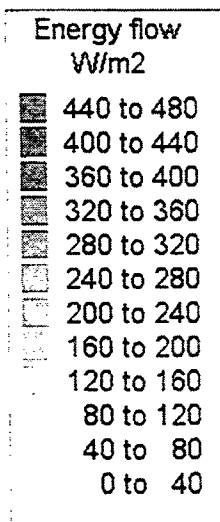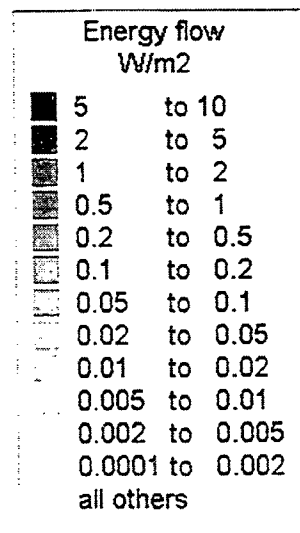
Energy flow W/m2
440 to 480
400 to 440
360 to 400
320 to 360
280 to 320
240 to 280
200 to 240
160 to 200
120 to 160
80 to 120
40 to 80
0 to 40

Figure 6.5. Scale used for solar radiation (W/m^2).

Figure 6.6. Scale of energy flow (to be used for energy production and use) (W/m^2).

Energy flow W/m2		
5	to	10
2	to	5
1	to	2
0.5	to	1
0.2	to	0.5
0.1	to	0.2
0.05	to	0.1
0.02	to	0.05
0.01	to	0.02
0.005	to	0.01
0.002	to	0.005
0.0001	to	0.002
all others		

In order to calculate the solar radiation incident on inclined surfaces, such as the ones characterising most solar panel installations, one would ideally need hourly data for direct and scattered radiation (or equivalently for direct and total global radiation). One would then assume that the scattered radiation is uniform to calculate its value for differently inclined surfaces. For the direct part, ray calculations with the appropriate angles between the direction to the sun and the normal to the collector surface have to be performed hourly. Such calculations have been performed and compared with measurements on inclined surfaces at several major solar installations and some weather stations (Sørensen, 1979,

2000). Here global data are needed and only monthly average radiation data are readily available (at least with data sizes suitable for the present type of investigation), so an approximate relation has to be invoked.

For use in connection with predictions of the energy production from solar collectors, the aim is to estimate the radiation on a surface tilted towards either North or South by an angle approximately equal to the latitude (as this gives the optimum performance) from the horizontal surface solar radiation data available. No great accuracy is aimed at, because actual solar panel installations are either

• Building integrated panels that will anyway be influenced by the structures at hand: Some solar panels will be mounted on vertical facades, others on roofs being either flat or tilted, typically by angles 30°, 45° or 60°. In all cases the orientation may not be precisely towards South or North, although one estimates the resource as comprising only those buildings facing approximately correct and not being exposed to strong shadowing effects from other structures. The penalty of incorrect orientation and tilting angle is often modest and mostly influences the distribution of power on seasons (Sørensen, 1979; 2000),

or

• Centralised solar farms that will generally be oriented in an optimum way, using total production maximising for panels not tracking the sun. However, the majority of locations suited for central solar installations are likely to be locations fairly close to the Equator, implying only modest seasonal variations in solar radiation, and the horizontal surface data are often quite representative.
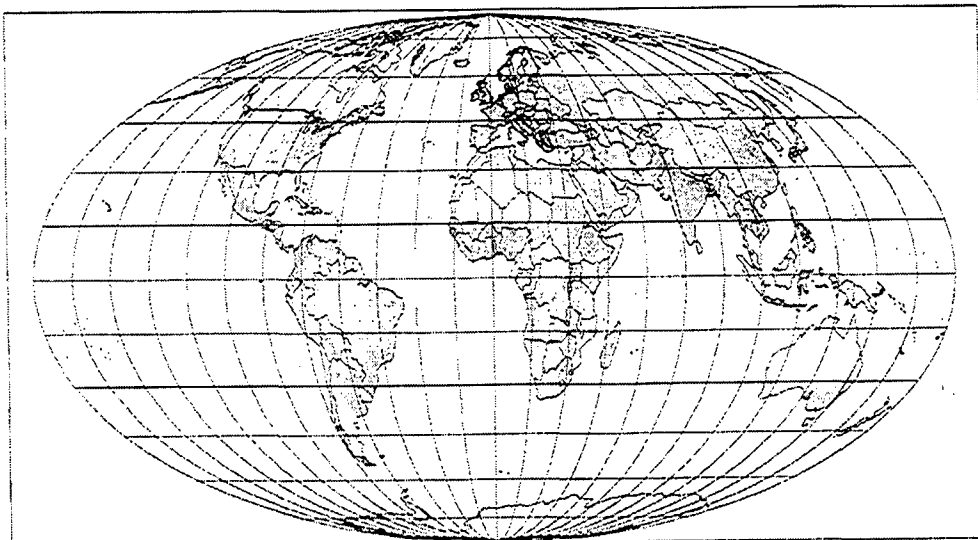

Figure 6.7. January potential energy production, originally calculated for building-integrated solar cells, with transmission and storage cycle losses subtracted. The potential thermal production would be about twice, again subtracting the losses in transmission and storage, which as described in the text are expected to be higher in this case (from Sørensen, 1999; scale given in Figure 6.6).
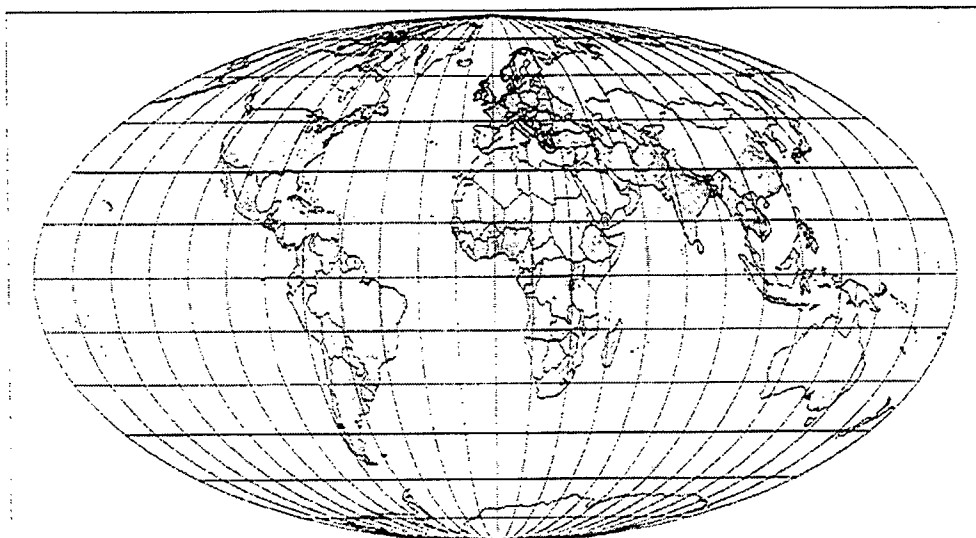
Figure 6.8. April and October potential energy production from building-integrated solar panels. The comments made in caption to Figure 6.7 applies (plain average of January and July values; from Sørensen, 1999; scale given in Figure 6.6).
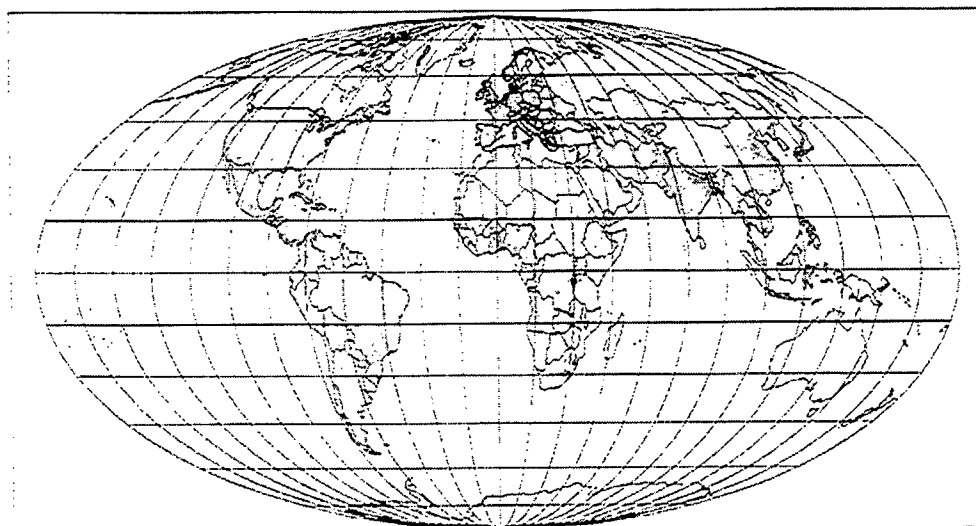

Figure 6.9. July potential energy production from building-integrated solar panels. The comments made in caption to Figure 6.7 applies (from Sørensen, 1999; scale given in Figure 6.6).
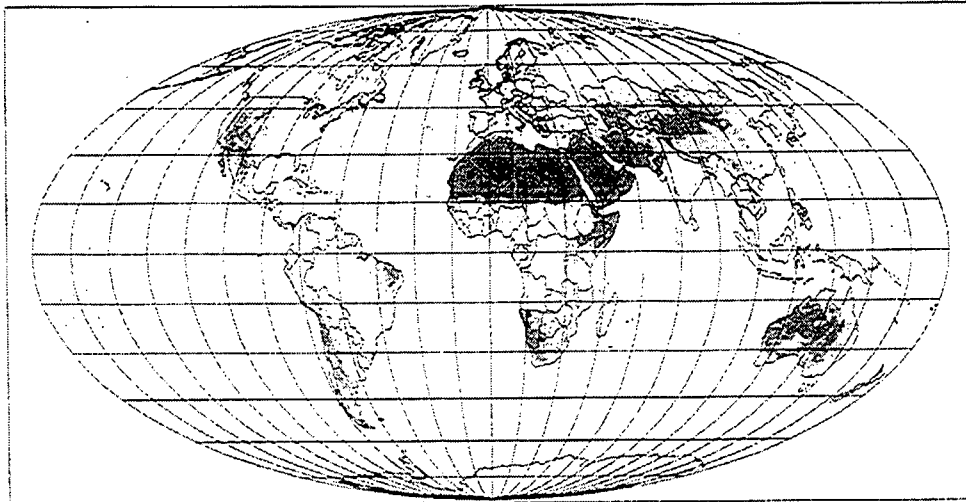
Figure 6.10. Potential annual average power production from centralised photovoltaic plants on marginal land, with transmission and storage cycle losses subtracted. Seasonal variations are modest (from Sørensen, 1999; scale given in Figure 6.11).
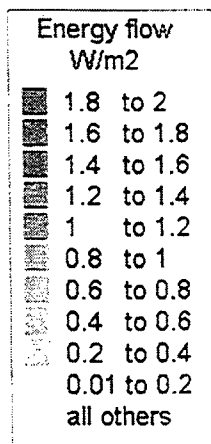
Energy flow
W/m2

- 1.8 to 2
- 1.6 to 1.8
- 1.4 to 1.6
- 1.2 to 1.4
- 1 to 1.2
- 0.8 to 1
- 0.6 to 0.8
- 0.4 to 0.6
- 0.2 to 0.4
- 0.01 to 0.2
- all others

Figure 6.11. Scale used for centralised photovoltaic production. Note that the scale is linear in contrast to the one used for decentralised power, e.g. in Figure 6.6 (W/m^2).

Due to of the many unknown factors regarding the precise inclination of actual installations; the following simple approximation is used (it originates from an analysis of the Danish latitude 56°N data by Sørensen, 1979): The radiation on a latitude-inclined surface in January and July are noted to be very nearly equal to the horizontal radiation in October and April, whereas the horizontal surface data for January and July are lower and higher than the inclined surface measurements, respectively. It is therefore decided to use the October and April horizontal data as a proxy for January and July inclined surface radiation, and construct the April and October inclined surface values as simple averages of the January and July adopted values. Furthermore, this procedure, which works well for the Danish latitude, will be less inaccurate for low latitudes, because of the relative independence of seasons mentioned above, and we simply use it for all locations.

The algorithm was originally set up to derive the energy extracted by photovoltaic solar panels, assuming a fixed conversion efficiency of 15%, which may be a fairly conservative estimate for future technology, considering that the current efficiency of the best mono-

crystalline cells is above 20% and that of amorphous cells near 10%, with multicrystalline cells falling in between. Future technology is likely to be thin-film technology, but not necessarily amorphous, as new techniques allow crystalline or multicrystalline material to be deposited on substrates without the complicated process of ingot growth and cutting. The efficiency of such cells is currently low, but as they are much less expensive than crystalline cells, they may be stacked in several layers and thereby still reach the efficiency envisaged here.

For thermal solar panels, the efficiency of the best current technology is about 60%. However, it depends on the inlet temperature, i.e. on the history of operating the system of collector and thermal storage cycle, e.g. through a water container. In order to reach efficiencies above 50%, it is necessary that the inlet temperature stays several ten's of degrees centigrade below the equilibrium temperature corresponding to the actual solar radiation intensity (i.e. the temperature at which temperature losses from the panel surface balances the radiative gain, cf. Sørensen, 1979; 2000).

Furthermore, the model estimates the availability of sites for mounting solar panels either in a decentralised fashion or centrally in major energy parks: The decentralised potential is based on availability of suitably inclined, shadow-free surfaces. It is assumed that the area of suitably oriented surfaces that may be used for building-integrated solar energy collection is 1% of the urban horizontal land area plus 0.01% of the cropland area. The latter reflects the density of farmhouses in relation to agricultural plot sizes and is based on European estimates, roughly assuming that 25% of rural buildings may install solar panels.

The potential photovoltaic production would thus be 15% of radiation times the fraction of the above two area types and the stated percentage for each, while the potential solar thermal production would be 60% of radiation times the same factors.

A final factor is applied in order to account for transmission and storage cycle losses. For photovoltaic, this is taken as 0.75, assuming about 5% transmission losses and that roughly half the energy goes through a storage facility of 60% round-trip efficiency (e.g. using a reversible fuel cells). For thermal hot-water systems, where the heat can often be used the same day as collected, these losses are typically 25-50%, giving a reduction factor of 0.5-0.75. For space heating systems at higher latitudes (where space heating is required), the losses can be much higher, a typical value for hot water storage in connection with detached one-family dwelling being 75%, implying a reduction factor of 0.2. This would not even be enough for high latitude systems aimed at 100% heat supply, because radiation during some months may be so low, that the storage system will have to be able to provide seasonal duration of heat storage. Other storage facilities, such as phase change stores, may perform better, but in any case the overall efficiency will be fairly modest.

The flow of energy reduced by all these factors represents the energy delivered to the end-use customers in the form of electricity or heat. It is shown in Figures 6.7-6.9 for each season (units in Figure 6.6), and with regional sums given in Table 6.1.

For centralised systems, the estimated potential is based upon 1% of all rangeland plus 5% of all marginal land (deserts and scrubland). Since these areas are nearly all very remote from heat load centres, the only sensible option is to produce electricity, which can then be transmitted to load areas and used for heat if necessary (presumable, this would make use of heat pumps). Therefore, only photovoltaic potential production will be estimated, using again as conversion efficiency 15% of the incoming radiation and a factor of 0.75 to account for transmission and storage losses. The resulting potential is shown in Figure 6.10 and Table 6.1.

It is seen that this is a huge amount of energy, and it shows that such centralised photovoltaic installations can theoretically cover many times the future energy demand.

Setting aside 1% of rangeland would imply an insignificant reduction in other uses of the land, even if this would rather be a small number of large photovoltaic installations. The same is true for desert and marginal land, where only the 5% most suited need to be invoked, which in reality might be 10% for the entire installation (including frames, access roads), of which the solar panels is only part. Because of the huge area of e.g. the Sahara desert this would suffice to supply more than the entire world need for energy. This would require the availability of intercontinental transmission, which may be quite realistic some time in the future, e.g. by use of superconducting trunk lines (Nielsen and Sørensen, 1996).

Table 6.1. Regional averages and sums of solar energy-supply related quantities (Sørensen, 1999).

Region (see below):	1	2	3	4	5	6	Total	unit
Area of region	20.1	15.4	28.3	26.3	20.1	30.9	141	M km^2
Urban area fraction	0.0063	0.0133	0.0096	0.0178	0.0290	0.0122	0.0147	
Rooftop solar thermal net energy potential:								
January	78	81	142	292	328	218	1140	GW
July	120	133	236	282	434	244	1448	GW
Annual average	99	107	189	286	380	230	1294	GW
Marginal land solar electric potential:								
January	2220	7310	6680	4500	7910	18200	46900	GW
July	3870	5990	9460	3980	11500	22700	57500	GW
Annual average	3040	6650	8070	4240	9690	20500	52200	GW

Regions: 1 = (United States, Canada), 2 = (Western Europe, Japan, Australia), 3 = (Eastern Europe, Ex Soviet Union, Middle East), 4 = (Latin America, South-East Asian "tigers"), 5 = (China, rest of Asia), 6 = (Africa).
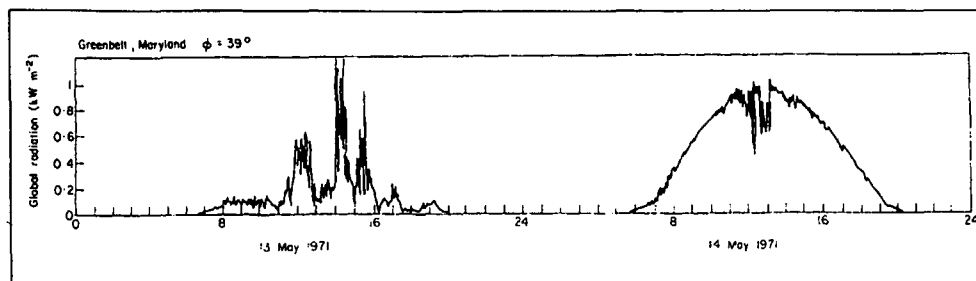Source: Sørensen (1999).

Figure 6.12. Two days of continuous record of total short-wavelength flux on a horizontal plane (based on Thekaekara, 1976).

An example of actual variations in solar radiation on a clear and an overcast day is shown in Figure 6.12, for a location in Maryland, USA, at 39°N (Thekaekara, 1976).

Regarding the variations in solar radiation on a horizontal plane with the hour of the day, there is a dependence which averaged over a month in summer and winter may look as shown in Figure 6.13 (based on long-term measurements at Hamburg, at 53.5°N, by Kasten, 1977). The downward short wavelength radiation is denoted E_{s+}^{sw}, the direct part D and the outgoing long wavelength radiation $R_s = E_{0-}^{lw}$. December mid-day radiation is at the selected urban location in many cases dominated by reflected radiation.
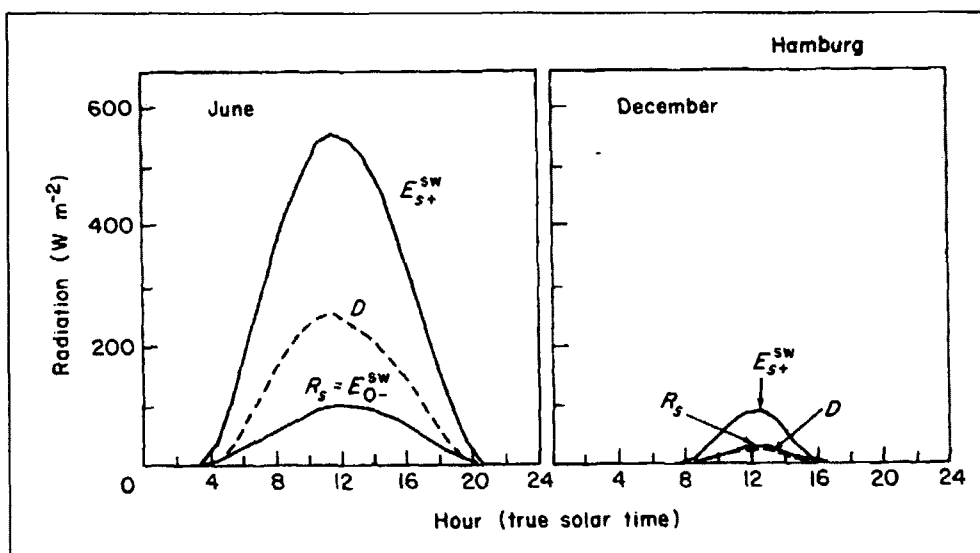

Figure 6.13. For the months of June and December, the total short-wavelength radiation on a horizontal plane at the Earth's surface in Hamburg is shown, and the direct and reflected radiation, for a given hour of the day. The fluxes are hourly averages based on 10 years of data, shown as functions of the hour of the day in true solar time (based on Kasten, 1977).
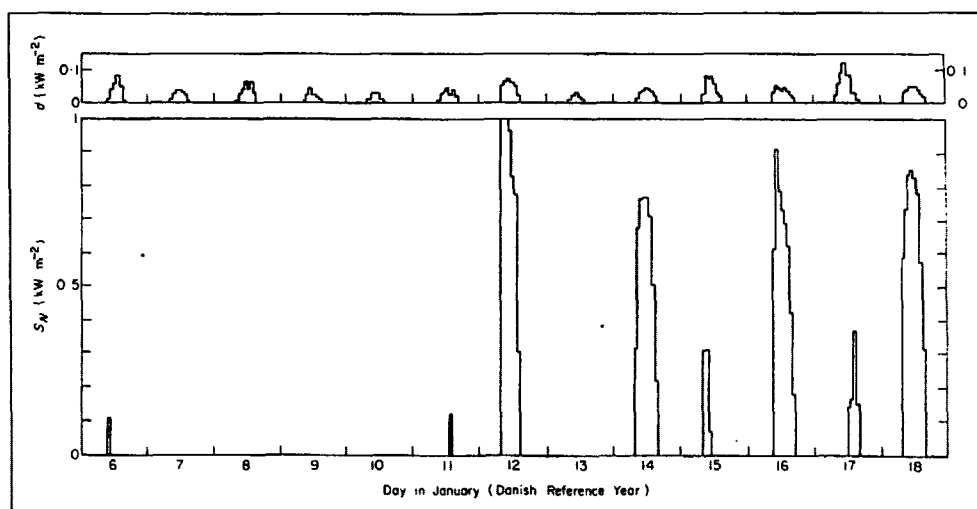

Figure 6.14. Hourly values of the normal incidence flux, S_N, and the scattered flux, d, on a horizontal plane, for the Danish reference year, $\phi = 56°N$. Thirteen consecutive winter days are shown (Sørensen, 2000).

An example of actual variations in direct and scattered radiation, hour by hour through several winter days for a location in Denmark at 56°N, is shown in Figure 6.14.

The components of the net solar radiation flux on a horizontal plane at the surface of the Earth do not have identical annual average values from year to year. In particular, the disposition of incoming radiation as rejected, scattered, direct and absorbed radiation is very sensitive to variations in cloud cover, and therefore exhibits substantial changes from year to year. Figure 6.15 shows the variations of yearly means of direct and scattered radiation measured at Hamburg (Kasten, 1977) over a 20-year period. Also shown is the variation of the net radiation flux at the ground. The largest deviation in direct radiation, from the 20-year average, is over 30%, whereas the largest deviation in scattered radiation is 10%. The maximum deviation of the net radiation flux exceeds 20%.
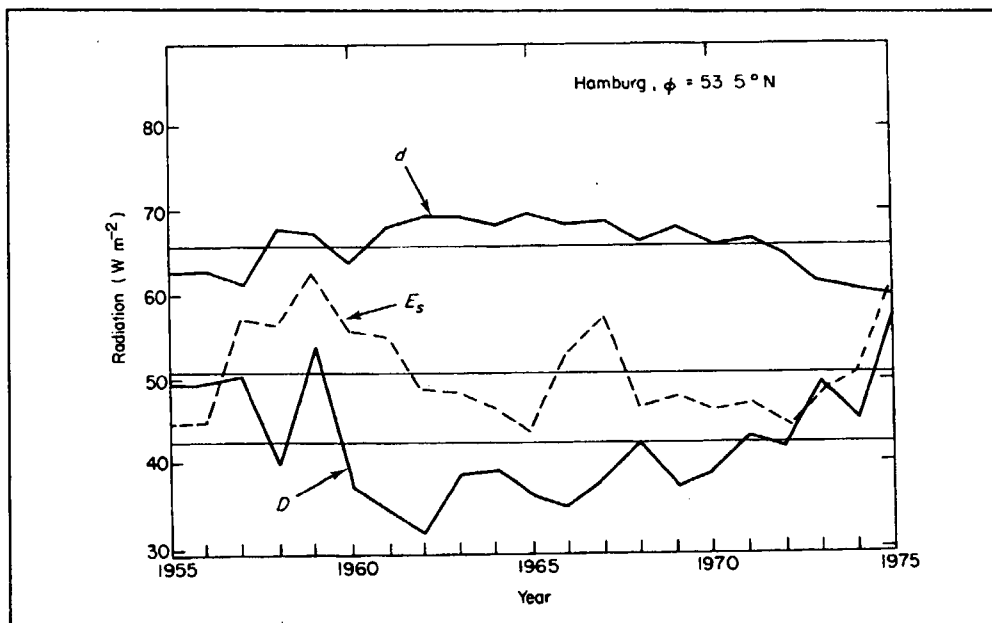

Figure 6.15. Variation of annual averages of direct and scattered radiation (solid, heavy lines) around their 21-year average value (thin, horizontal lines), for Hamburg. Also shown is the variation in net radiation flux (dashed line) around its 21-year average value. (based on Kasten, 1977).

One way of presenting the variability of solar radiation is through a power duration curve, which is an accumulated frequency distribution: it gives the fraction of time during which the energy flux exceeds a given value E, as a function of E. Figure 6.16 gives power duration curves for total and for direct radiation on a horizontal surface and two southward inclined surfaces, for a location at latitude $\phi = 56°N$ (Danish reference year, cf. European Union, 1985). Since data for an entire year have been used, it is not surprising that the energy flux is non-zero for approximately 50% of the time. The largest fluxes, above 800 Wm^{-2}, are obtained for only a few hours a year, the largest number of hours with high incident flux being for a surface inclined about 45°. The shape of the power duration curve may be used directly to predict the performance of a solar energy device, if this is known to be sensitive only to fluxes above a certain minimum value, say 300 Wm^{-2}. The power duration curves for direct radiation alone are shown on the right. They are relevant for devices sensitive only to direct radiation, such as most focusing collectors.
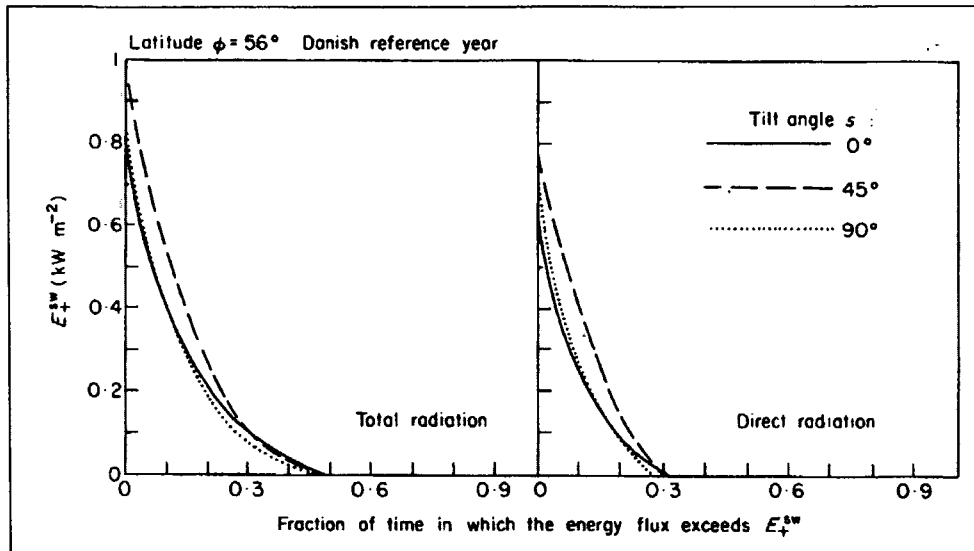
Figure 6.16. One–year power duration curves of total and direct (right-hand side) short-wavelength radiation on south-facing surfaces of three different inclinations, based on the Danish reference year, $\phi = 56°$N (Sørensen, 2000).
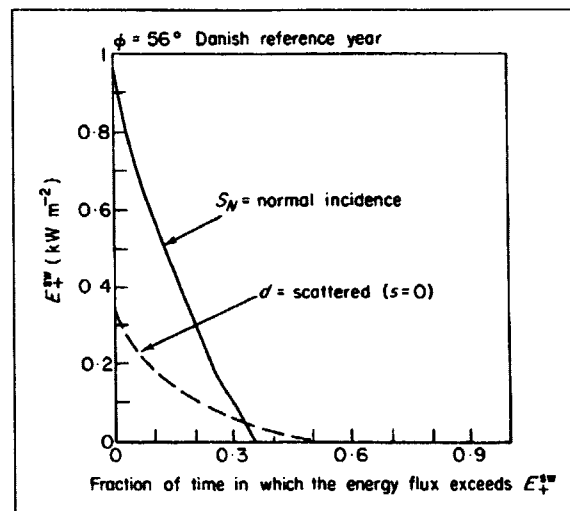

Figure 6.17. One–year power duration curves of normal incidence radiation alone, and of scattered radiation alone, based on the Danish reference year ($\phi = 56°$N). The normal incidence curve would correspond to the radiation received by a fully tracking instrument. The curve for scattered radiation is for a horizontal surface (Sørensen, 2000).

Figure 6.17 gives the power duration curves for normal incidence radiation, S_N, and for scattered radiation on a horizontal plane, d. The normal incidence curve is of interest for fully tracking devices, i.e. devices which are being continuously moved in order to face the direction of the Sun. By comparing Figure 6.17 with Figure 6.16, it can be seen that the

normal incidence curve lies substantially above the direct radiation curve for an optimum but fixed inclination ($s = 45°$). The power duration curve for normal incidence radiation is not above the curve for total radiation at $s = 45°$, but it would be, if the scattered radiation received by the tracking plane normal to the direction of the Sun were added to the normal incidence (direct by definition) radiation. The power duration curve for scattered radiation alone is also shown in Figure 6.17, for a horizontal plane. The maximum scattered flux is about 350 Wm^{-2}, much higher than the fluxes received during winter days.

The examples given above of time variations of solar radiation at different time-scales have given an impression of the complexity of the storage issue. To arrive at a prescription for dealing with these variations, also the load variation must be established.

6.2.2 Heat demand

The use of heat depends on the size of population and in case of space heating on the climatic conditions. The current use of space heating and other form of heat is estimated in Table 6.2, for major regions of the world. Space heating is calculated on a geographical basis by the method described below. The other entries are taken as proportional to population density and reflect the goal satisfaction assumed to be characterising each region in 1994. This concept is introduced in order to produce realistic predictions of future demand, as shown in Tables 6.3 and 6.4.

Table 6.2. Regional analysis of annual average end-use heat energy flow in 1994 (for definition of regions, see notes to Table 6.1). Population and area data are also given (Sørensen, 1999).

Region:	1.	2.	3.	4.	5.	6.	Average and total	unit
Space heating	186	207	61	2	19	1	46	W/cap
	52	116	41	1	48	1	260	GW
Other low-T heat	120	130	40	15	18	10	36	W/cap
	34	73	27	12	47	7	199	GW
Medium-T heat	40	50	30	10	10	5	17	W/cap
	11	28	20	8	26	3	97	GW
High-T heat	35	40	30	10	10	3	16	W/cap
	10	22	20	8	26	2	88	GW
Population 1994	282	561	666	820	2594	682	5605	million
Region area	20	15	28	26	20	31	141	million km^2

The definition of "end-use" should first be clarified, as this concept is vague: The difficulty derives from the difference between the energy delivered to the end-use, to be converted in order to satisfy his or her demand, and the end-use energy defined as that actually contributing to satisfying the real need, which of course is not energy. As an example take lighting. A light bulb gives a certain number of lumens per watt and since the final demand is light, the end-use energy should be the energy in the light and not the electricity feeding into the bulb. Current compact fluorescent bulbs provide close to 50 lm/W, implying a final energy conversion efficiency of about 10%. The intention behind the end-use figures given in Table 6.2 and the following tables is to give the end-use energy provided by current state-of-the-art technology. Thus, if the average delivered power required for satisfying a

13

person's lighting needs is 10W, then the end-use energy will be entered as 1W. For space heating, the end-use energy for a building is taken as the losses through outer surfaces, for a building with state-of-the-art insulation and glazing. The precise amount assumed per capita is described below.

The end-use energy demands for heat and other forms of energy may generally be distributed on energy qualities categorised as follows (Sørensen, 1999; 2000):

1. Cooling and refrigeration 0-50°C below ambient temperature.
2. Space heating and hot water 0-50°C above ambient.
3. Process heat below 100°C.
4. Process heat in the range 100-500°C.
5. Process heat above 500°C.
6. Stationary mechanical energy.
7. Electrical energy (no simple substitution possible).
8. Energy for transportation (mobile mechanical energy).
9. Food energy.

The goal categories used to describe basic and derived needs have been chosen as follows (Kuemmel *et al.*, 1997):

A: Biologically acceptable surroundings
B: Food and water
C: Security
D: Health
E: Relations and leisure
F: Activities
    f1: Agriculture
    f2: Construction
    f3: Manufacturing industry
    f4: Raw materials and energy industry
    f5: Trade, service and distribution
    f6: Education
    f7: Commuting

Here categories A-E refer to direct goal satisfaction, f1-f4 to primary derived requirements for fulfilling the needs, and finally f5-f7 to indirect requirements for carrying out the various manipulations stipulated.

Among the heat-related demands are space conditioning (being part of biologically acceptable surroundings). This is estimated using the following considerations:

Suitable breathing air and shelter against wind and cold temperatures (or hot ones) may in some circumstances require energy services, indirectly to manufacture clothes and structures, or directly to provide active supply or removal of heat. Insulation by clothing makes it possible to stay in cold surroundings with a modest increase in food supply (which serves to heat the layer between the body and the clothing). The main heating and cooling demands occur in extended spaces (buildings and sheltered walkways, etc.) intended for human occupation without the inconvenience of heavy clothing that would impede e.g. manual activities.

Space heating is assumed to be required if the monthly average temperature is below 16°C. This would give an indoor temperature above 20°C in a suitably constructed buildings, taking into account thermal mass (to smooth out day-to-night temperature

variations) and indoor activities producing waste heat. Space cooling is considered necessary for monthly average temperatures above 24°C, again with consideration of optimum use of storage in building thermal mass and devices such as smart solar window screens.

The rate of energy provision for heating and cooling is calculated from the temperature difference ΔT by the simple formula $P = C \times \Delta T$ (Sørensen, 1979), where C=36 W/cap/K. assuming an average heated or cooled space of 60 m² per person (40 m² living space, the rest for work and public spaces). Just under 60% of the space heating cover heat losses through external walls, the rest is air exchange, partially through heat exchangers.

Figure 6.18-6.21 (scale in Figure 6.22) shows the measured seasonal temperatures (taken from Leemans and Cramer, 1998; the data are consistent with other sources such as NCEP/NCAR, 1998) and indicates the seasonal movements of the borders defining the onset of needs for space cooling or space heating.

Figure 6.23-6.26 (scale in Figure 6.27) gives the energy per unit of populated land area required in 2050 for full satisfaction of heating needs. It is the quantity |P| defined above times the population density for 2050.

Table 6.3. Per capita heat end-use annual average energy flow for "full goal satisfaction" (in W/cap.; Sørensen, 1999).

Regions (cf. Table 6.1):	1.	2.	3.	4.	5.	6.
Space heating*	201	186	191	7	225	10
Other low-temp. Heat	150	150	150	150	150	150
Medium-temp. Heat	50	50	50	50	50	50
High-temp. Heat	40	40	40	40	40	40

* These rows are evaluated on the basis of temperature data in each GIS cell.

Table 6.4. Fraction of "full goal satisfaction" assumed for 2050 scenario (estimated values for 1994 given for comparison, in parentheses) (Sørensen, 1999).

Regions:	1.	2.	3.	4.	5.	6.
Space heating	0.9	1.0	0.75	0.67	0.63	0.15
	(0.9)	(0.96)	(0.25)	(0.08)	(0.16)	(0.10)
Other low-temperature	0.87	1.0	0.53	0.6	0.67	0.13
heat	(0.8)	(0.87)	(0.27)	(0.10)	(0.12)	(0.07)
medium-temperature heat	0.9	1.0	0.8	0.8	0.8	0.1
	(0.8)	(1.0)	(0.6)	(0.2)	(0.2)	(0.1)
High-temperature heat	0.88	1.0	0.75	0.75	0.75	0.13
	(0.88)	(1.0)	(0.75)	(0.25)	(0.25)	(0.08)

In Table 6.3, the regional totals of the estimated per capita heat requirements for full satisfaction of the associated needs are shown, the assumed space heating of 60 m² floor space per capita in countries presently near full satisfaction of shelter demands corresponds to 40 m²/cap. for dwelling and 20 m²/cap. for work). The global temperature maps of

Figures 6.18-6.21 were used to determine the amounts of heat required, for an insulation-wise state-of-the-art building. The other heat demands given in Table 6.3 are estimated as climate-independent. Table 6.4 gives the fractions of "full goal satisfaction", that on average has been achieved at present (1994-values), together with future values expected for different regions (these are used in a range of scenarios for the mid-21st century developed in connection with the greenhouse damage mitigation work described e.g. in Sørensen (1999)).
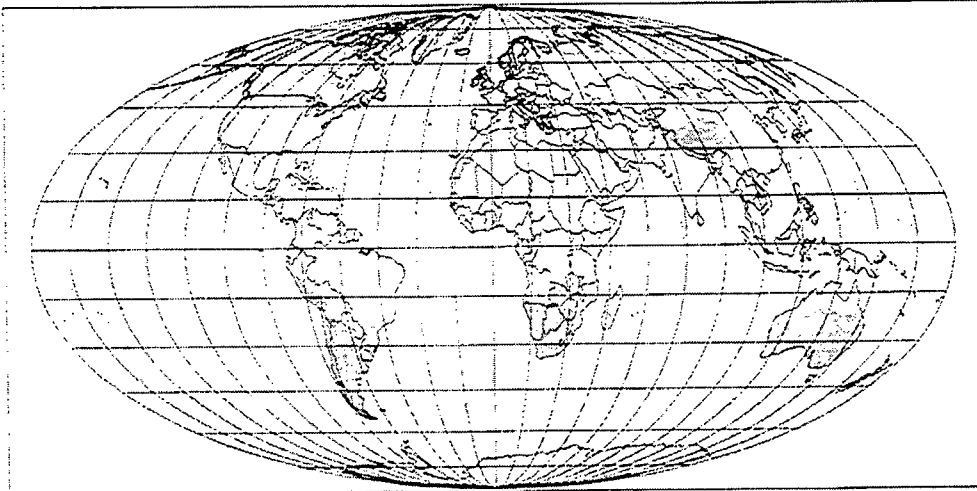
Figure 6.18. January average temperatures indicating areas with space heating and cooling needs (data source: Leemans and Cramer, 1998; the scale is given in Figure 6.22).
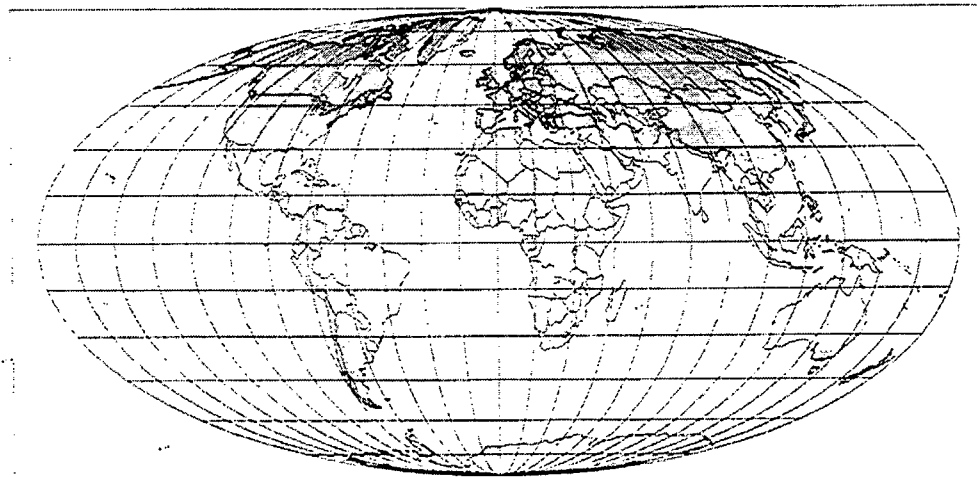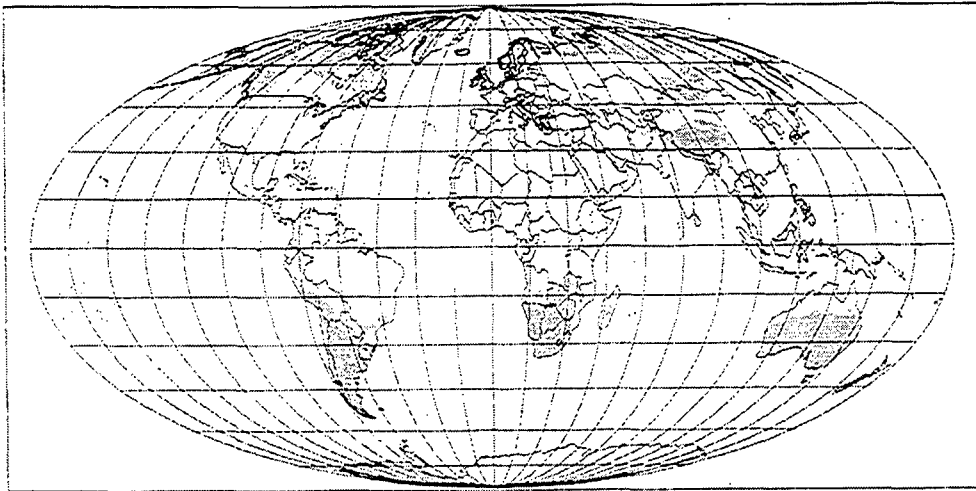

Figure 6.19. April average temperatures indicating areas with space heating and cooling needs (data source: Leemans and Cramer, 1998; the scale is given in Figure 6.22).
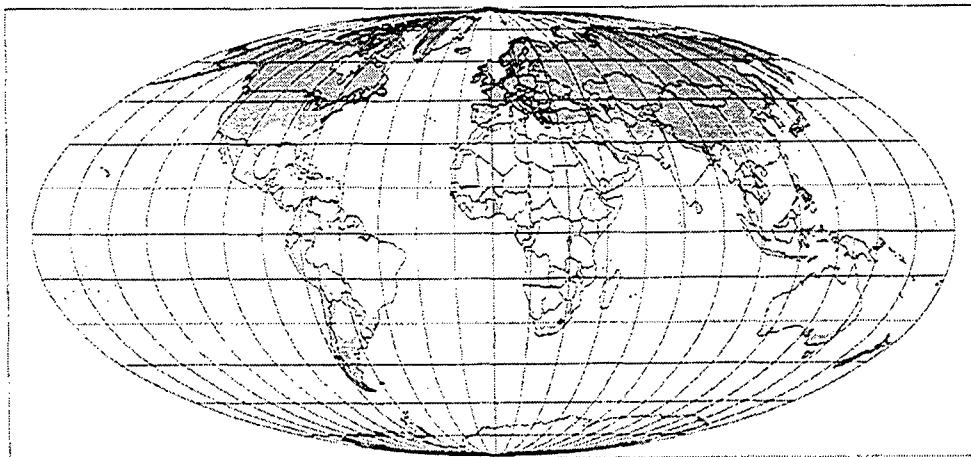
Figure 6.20. July average temperatures indicating areas with space heating and cooling needs (data source: Leemans and Cramer, 1998; the scale is given in Figure 6.22).

Figure 6.21. October average temperatures indicating areas with space heating and cooling needs (data source: Leemans and Cramer, 1998; the scale is given in Figure 6.22).

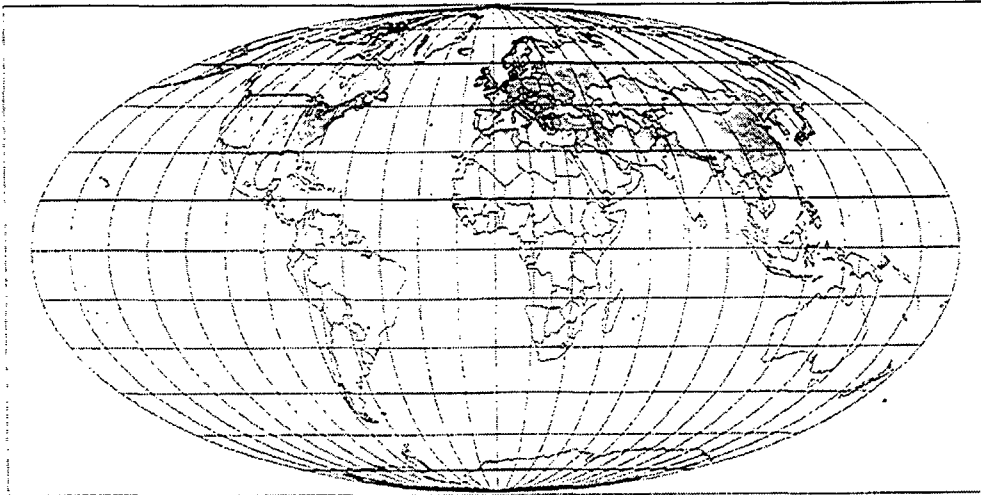| Temperature deg. C |
| --- |
| 32 to 40 |
| 24 to 32 |
| 16 to 24 |
| 8 to 16 |
| 0 to 8 |
| -10 to 0 |
| -20 to -10 |
| -30 to -20 |
| -50 to -30 |

Figure 6.22. Temperature scale (deg. C)

Figure 6.23. January space heating energy requirements for full satisfaction of indoor comfort needs (scale given in Figure 6.27).
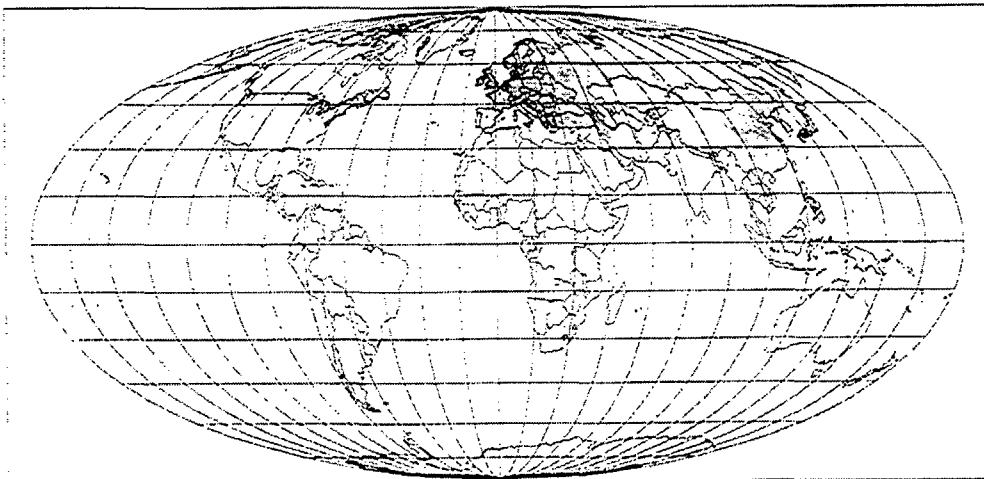

Figure 6.24. April space heating energy requirements for full satisfaction of indoor comfort needs (scale given in Figure 6.27).
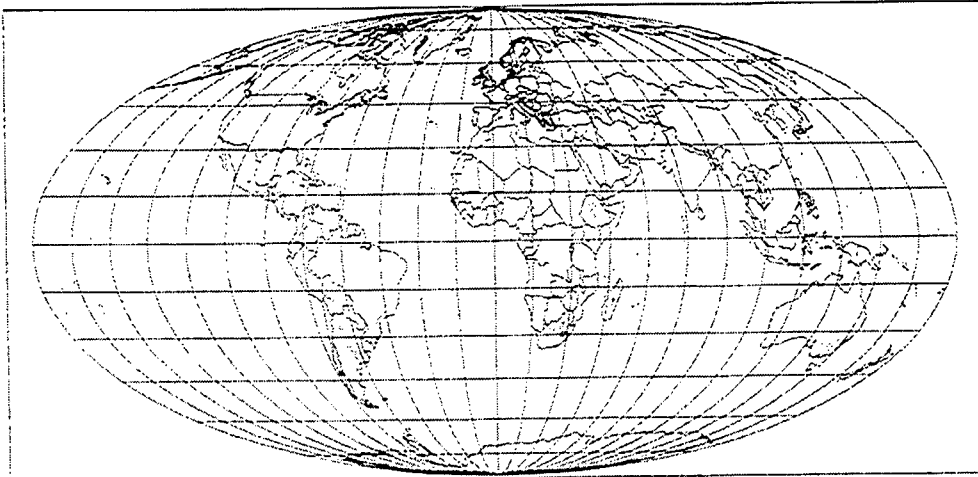
Figure 6.25. July space heating energy requirements for full satisfaction of indoor comfort needs (scale given in Figure 6.27).
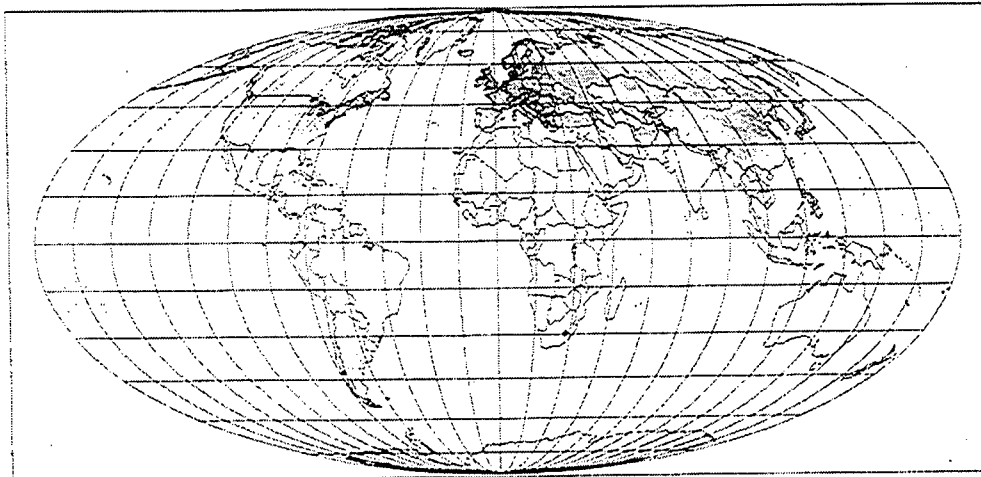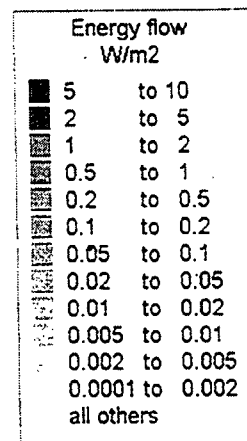

Figure 6.26. October space heating energy requirements for full satisfaction of indoor comfort needs (scale given in Figure 6.27).

Figure 6.27. Scale of energy flow (rate of energy capture, conversion or use, note that the scale is logarithmic) (W/m²).

Energy flow W/m2		
5	to	10
2	to	5
1	to	2
0.5	to	1
0.2	to	0.5
0.1	to	0.2
0.05	to	0.1
0.02	to	0:05
0.01	to	0.02
0.005	to	0.01
0.002	to	0.005
0.0001	to	0.002
all others		

19

6.2.1 Matching requirements

Comparing the solar heating potentials given for the four seasons in Figures 6.4 to 6.7 with the demands for space-heating in Figures 6.23-6.27, one sees that there is insufficient decentralised solar energy (i.e. from building-integrated installations) during fall and winter in many of the high-load areas, notably in the Northern hemisphere. The patterns of shortfall indicates that if the problem is to be overcome by storing solar heat from periods of surplus to periods of deficit, then the average storage time increases with latitude, reaching up to a half year in several populated areas.

The implication of this observation is, that if low-temperature heating is to be provided by thermal solar collectors alone, then substantial amounts of long-term storage facilities must be part of the system. The geographical pattern shows that it is not sufficient to just increase the capacity of the solar collectors to be adequate for the period of least radiation (and then presumably having to discard the surplus energy in the most favourable season). At the higher, populated latitudes, there simply is so little radiation during part of the winter, that it is not practical to proceed in this manner: storage must be added, or some alternative heat source without the seasonal mismatch must be part of the system. At lower latitudes, the problems diminish, but in the most populated areas of the world (Europe, Asia and North America) there is still a considerable out-of-phase seasonal variation in both heating demand and in solar radiation. Therefore, it is also in these regions likely to be a sound solution to add some heat storage capacity, rather than just increase the solar collection area. As one moved towards the Equator, the size of the required heat store declines from seasonal to monthly or weekly. For systems aiming only at providing hot water at low latitudes, it is often sufficient to have storage facilities for 1-2 days of storage.

Since not all the renewable energy sources have a seasonal variation out-of-phase with the heat demand, there are possibilities of combining different kinds of renewable energy and thereby diminish or eliminate the need for storage. The first is the case for combination with wind power, while the last may be true for combinations with biomass energy systems (based on storable biomass products) or hydro power with seasonal water reservoirs. Most of these alternative resources most easily produce electricity (as direct solar radiation may also do if harvested by photovoltaic panels), rather than heat, and it is therefore relevant to rethink the options for providing heat in this case. Low-temperature heat has a low thermodynamic energy quality (as indicated by second law efficiencies), whereas electric power has high thermodynamic efficiency and thus offers more possibilities of "smart" system design.

One obvious option is to employ heat pump technologies and thereby divide the energy input into a smaller fraction of high-quality energy, plus a larger fraction of low-quality energy, that may be environmental heat (from air, soil or waterways) or heat from a solar thermal collector unable to raise the water temperature enough.

Figure 6.28 gives the electric energy input to heat pumps for providing space heating, hot water and other low-temperature heat demand for the high goal satisfaction scenario outlined in section 6.2.2 above, on a geographical basis corresponding to the total regional heat uses implied by the numbers given in Table 6.3 and 6.4. A fairly low average COP (coefficient of performance, i.e. ratio of heat output to electricity input) of 3.33 has been assumed for the heat pumps, because the majority of them will be placed at high latitude locations (where the space heating need is largest). At these locations they will in most cases need soil sources and corresponding technology for the low-temperature source. Current technology uses pipes shot through the earth at frost-free depths by special

machinery to extract this heat, and the rather low COP is an indication of the average current performance of such systems in cold climates.
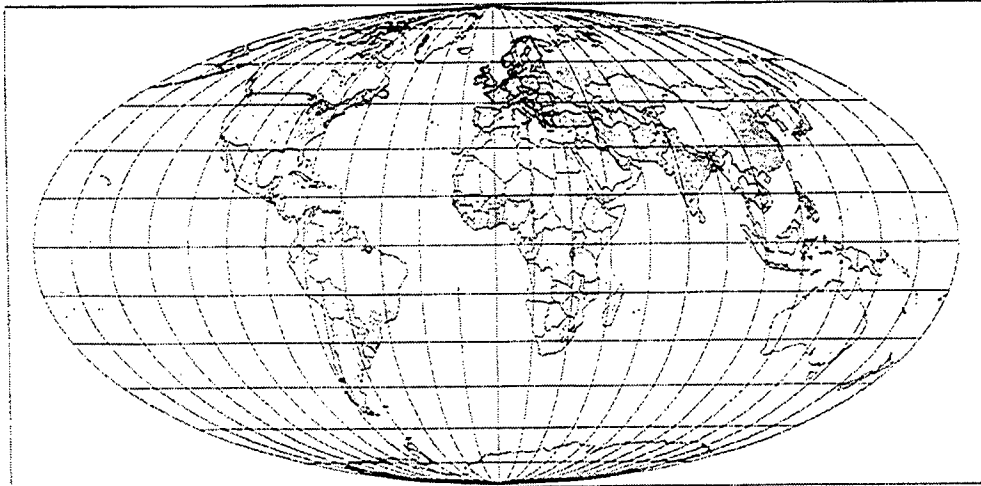

Figure 6.28. Required annual average energy input to heat pumps used for producing space heating, space cooling and other low temperature heat, to be delivered to consumers in high goal satisfaction scenario for the mid-21st century (scale given in Figure 6.27). Annual averages were constructed from January, April, July and October data and may differ slightly from the 12-month averages.

6.3   Heat storage systems operating with renewable energy

Simple hot water storage systems are parts of nearly all central heating installations today, as well as of many systems in more primitive surroundings, down to a stand-alone black container heated during the day and providing water for a bath in the evening, a system commonly seen in areas with little organised energy delivery.

Buildings themselves can be regarded as heat stores. In climates with hot days and cool nights, building thermal mass is used to diminish daytime indoor temperatures and increase nighttime temperatures. For hot climates without strong day-to-night temperature differences, the building design solution may be the same as in generally cold climates, i.e. to insulate walls and reduce transmission through glazing. Typical wall insulation thickness in new houses currently built at high northern latitudes is 25 cm, with losses through windows under 1 $Wm^{-2}K^{-1}$.

Building design optimisation involves appeal to both passive solar techniques and passive thermal storage methods. In case renewable energy systems such as solar thermal collectors, or photovoltaic cells with cooling circuits (also called combined thermal and electric solar collection systems), are used, there are special requirements for low-temperature thermal storage. Concentrating solar thermal collectors may be operated at higher temperatures, and the corresponding energy stores thus selected from the broader set of options available in that case (Sørensen, 2000). While short-term storage at low temperatures is mostly done using thermal heat capacity stores, seasonal storage using heat capacity involves losses, even if insulated surface-to-volume ratios are diminished by going to large systems, and alternatives such as phase-change stores may thus be considered.

Existing solar thermal systems are generally of the following categories: Thermosyphon systems for hot water provision in low latitude locations, forced circulation systems for hot water and space heating at higher latitudes, and communal systems for feeding into district heating lines. Storage requirements for these systems range from modest to massive, and in many cases, the alternative of a backup supply system is chosen.
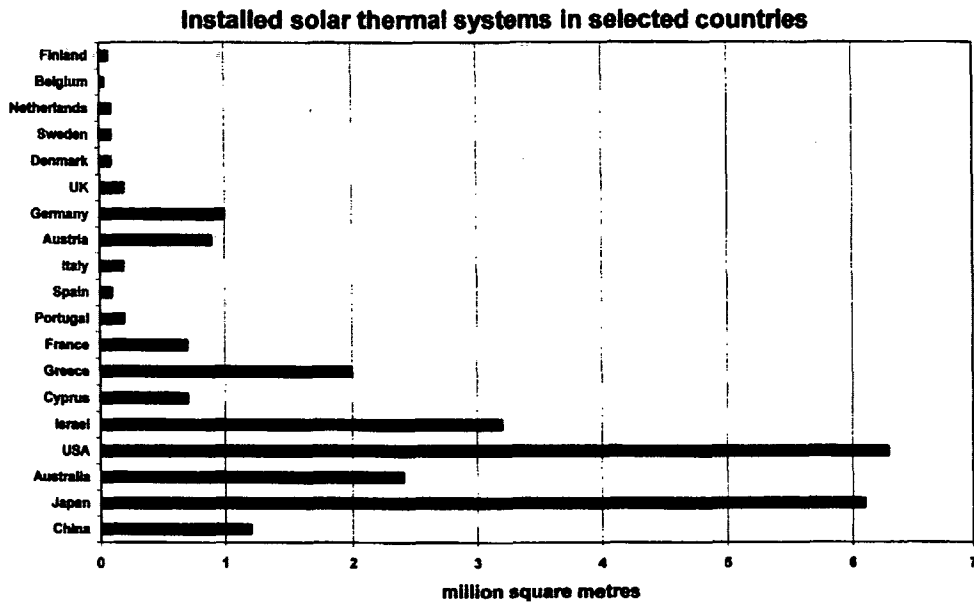
Installed solar thermal systems in selected countries

Figure 6.29. 1995 installed solar thermal collector areas in selected countries (European Solar Industry Federation, 1996 and Lamaris, 1997).

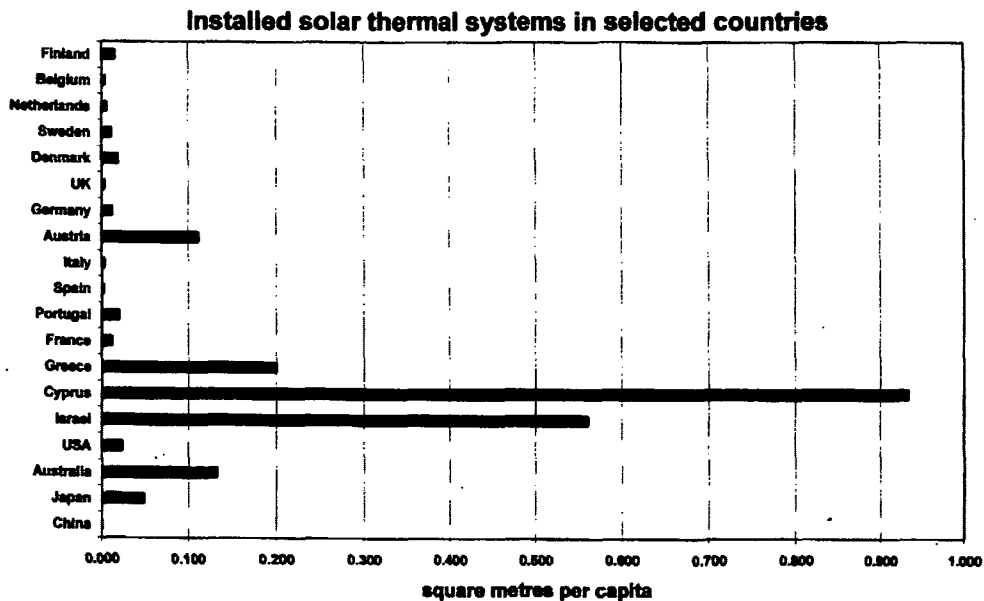**Installed solar thermal systems in selected countries**

Figure 6.30. Same as Figure 6.29, but per capita.

Figure 6.29 shows the installed areas of solar thermal collectors in selected countries, and Figure 6.30 the same on a per capita basis. Most of the collector area is in small single-dwelling rooftop systems (performance data for selected houses may be found in Balcomb et al, 1996), but a few percent represent demonstration plants with ground-based collector fields, and in some cases either communal storage or attachment to a district heating system, for which the solar heat is usually a tiny fraction of the total heat generated. A number of larger systems operating in Europe are collected in Figure 6.31.
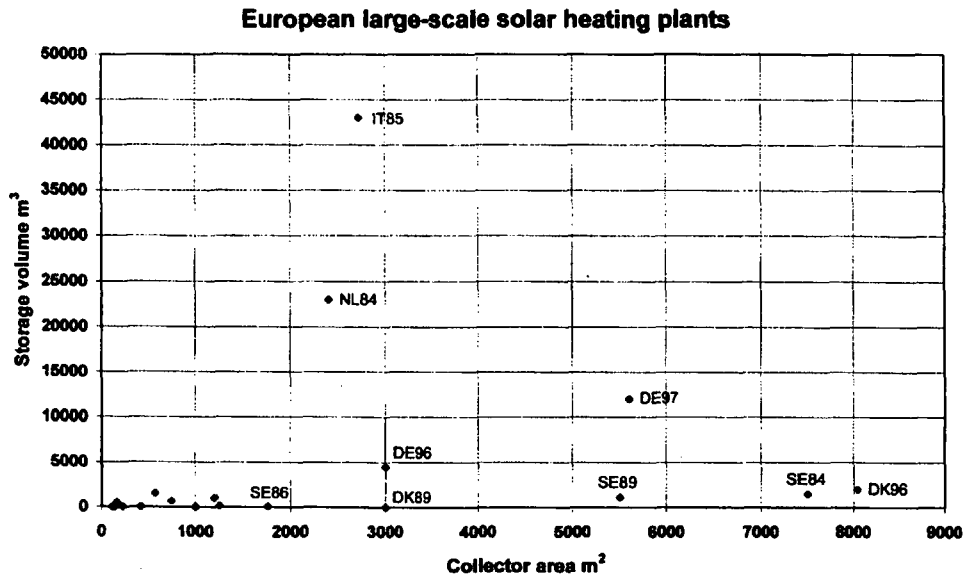

European large-scale solar heating plants

Figure 6.31. Storage volume to collector area ratios for 1997 stock of large-scale European solar thermal systems (Fisch et al., 1998; Dalenbäck, 1997). Labels give country (IT=Italy, NL=Netherlands, DE=Germany, DK=Denmark, SE=Sweden) followed by year of installation.

It is seen that the high-latitude Scandinavian countries have tested large collector area systems, but not systematically aimed at seasonal storage as a required option. The largest existing system, located in Denmark, integrates small quantities of solar thermal (about 10%) into an existing fuel-based system distributing heat through district heating lines (Blarke, 1997). The attached 2000 m^3 heat store is only for short-term smoothing purposes. In Italy, the Netherlands and Germany, attempts to test seasonal storage are carried out, although the systems listed are not reaching more than around 70% overall solar coverage.

The high-latitude installation in Sweden (denoted SE84 in Figure 6.31) receives an annual average solar radiation of 119 Wm^{-2} of which 29% is delivered to the users. Due to the small size of the heat store, storage losses are only 5%. During the season 1987/88, the solar heat constituted 6.5% of the total demand by the users (Isakson, 1989). The March-to-October average temperature in the solar panel circuit was 64·°C, that at the entrance to the heat store 60 °C, and the temperature of heat drawn from the exit of the heat store 54 °C.

The corresponding numbers for an installation at medium latitudes are in case of a 91 m^2 thermal collector system based on evacuated tube panels, with a 500 m^3 water store, at University of Calabria, Italy (Oliveti et al., 1998), are: Annual average solar radiation on collector: 184 W/m^2, overall efficiency of heat delivery: 28%, with an average primary

collector efficiency of 53%. Most of the losses are from the heat store, but a few percent from piping. This system covers 100% of heat demand in the 1750 m³ building, being designed for the winter conditions.

Storage systems other than heat capacity storage (and most often in water) have been investigated on smaller scales, notably phase change stores. However, they have not reached commercial viability, despite considerable effort (Bakken, 1981).

6.4   Simulation of system performance

In most countries using solar thermal energy, software has been developed to simulate the system performance and allow engineering design of suitable systems for particular requirements.

As an example, Figure 6.32 shows the monthly simulation results for the full coverage Italian system described above. The software called COSIMI solves instantaneous balance equations and treats the store as an entity without thermal stratification. Yet the overall behaviour is quite similar to the measured one (Oliveti et al., 1998).
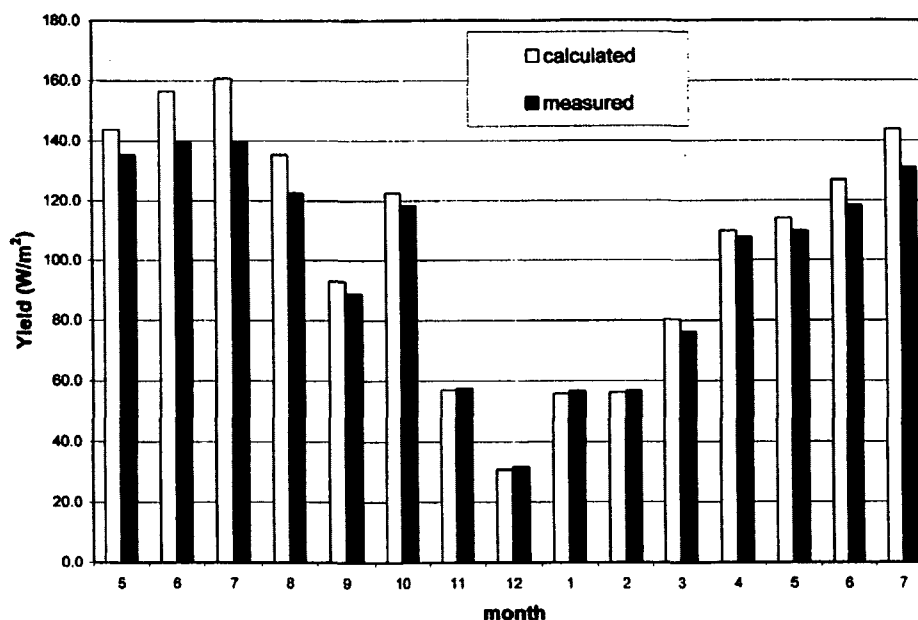

Figure 6.32. Calculated and measured collection of solar energy 1995-1996 for University of Calabria system, using simulation of collection, collector loop and storage loop, with irradiation and heat use data given as the measured ones (Oliveti et al., 1998).

S. Klein as described in Duffie and Beckman (1974) set out the basic assumptions used in simulation of thermal collector performance. It includes an analytical approximation for transmission and absorption in cover glass layers and absorber (allowing many reflections back and forth), and a linear approximation for the heat transmission through the collector, as is commonly used for other heat losses through the building shell. Refinements include treatment of dynamical behaviour (Hilmer et al., 1999). Considerable effort has been made

to validate models against measurements, considering not only limitations of models but also uncertainty of data collection (Mathioulakis *et al.*, 1999).

Figure 6.33 gives the simulated performance of a solar thermal system mounted on a 45° roof of a detached one-family dwelling located at 56°N, using the software described in Sørensen (1976). Despite fully covering the south-facing roof with 60 m² of solar collectors, and adding a 40 m³ water storage in the basement, it is seen that auxiliary energy is still required during 30-40% of the year. The parameters used in the simulation are shown in Table 6.5. They also indicate the types of effects included in the model simulation.

Solar radiation data and ambient temperatures were taken for the Danish Reference Year, an hourly data set composed of real data sequences from different years, put together in such as way that both monthly averages and short-term variations are near their long-term values. The hour-by-hour simulation covered one year and it was required that the state of the system at the end of the simulation year was roughly identical to the condition assumed at the beginning of the year. In this way, the calculation could have been continued cyclically. The particular parameter that has to be adjusted in order to achieve this is the initial temperature of the water in the storage tank. In other words, all the simulation calculations presented are characterised by giving a storage temperature at the end of the year, which is identical to the one chosen at the beginning of the year.

The parameters for the simulation, shown in Table 6.7, indicates a 60 m² solar collector placed on a south-facing rooftop tilted 45°, with one layer of glazing, a selective surface on the absorber plates, and a 40 m³ water storage with a heat loss coefficient $U_s = 13.5$ W °C^{-1}, corresponding to about 0.2 m of rockwool insulation, if the shape of the tank is a half sphere (area $3\pi R^2$, R being the radius).

The results of the simulation are displayed in Fig. 6.33, in the form of monthly average values. The energy fluxes selected for display are the gain from the collector, the energy drawn from the storage (to the load areas), the insulation losses from the storage, and the auxiliary heat needed, i.e. the loads which could not be covered by solar energy. The situations requiring auxiliary energy are those in which the temperature of the storage is below 45°C, which is the assumed minimum temperature $T_{L,in}$ for the water entering into the load circuit, as well as the required hot water temperature (assumed to be 40°C above a fixed water temperature provided by the waterworks).

For hot water, the water from the waterworks is first raised to the storage temperature T_s, and the auxiliary energy required is thus that needed to raise the temperature further, from T_s to 45°C. The heat exchange between storage and hot water flow has been assumed to be perfect.

For the remaining load, the transfer medium is assumed to be in the form of hot water circulating between storage and load areas ("radiators"). Again, it is assumed that the storage can raise the temperature of the water in the load circuit to T_s. If this is below 45°C, auxiliary heating is applied in order to bring the temperature up to 45°C. The temperature drop through the load circuit is taken as 15°C.

Systems based on air circulation to the load areas, or on covering a part of the space heating need by hot water pipes in the (say concrete) floors, would be characterised by a minimum temperature requirement lower than 45°C, typically 30–35°C. It would thus seem that such floor heating systems would be more suitable in connection with solar heating systems, where the storage temperature may be in the range 30–45°C during an important portion of the year. Air circulation systems are also typically characterised by larger temperature losses in heat exchangers, owing to the low heat capacity of air, or alternatively by high circulation speeds, which may entail other undesirable features (noise, non-negligible use of electric energy for circulation fans, etc.). Floor heating systems are

usually characterised by slow response to regulation, and peak loads must in some cases be covered by a separate system (e.g. hot water radiators with a temperature of at least 45°C, as compared with the 30°C typically used in the floor pipes).
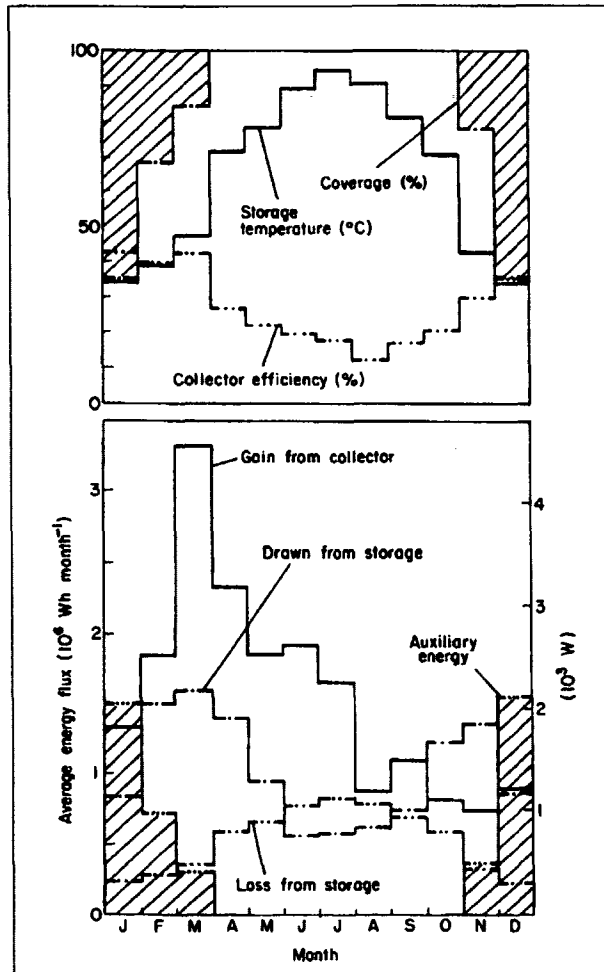

Figure 6.33. Simulation results for Danish one-family dwelling (Sørensen, 1979).

Figure 6.33 shows the annual total amount of auxiliary energy needed in the Danish case as 26.7% of the net load. The figure illustrates a typical problem in connection with solar heating systems aimed at covering a large part of a heating requirement, the seasonal variation of which is "anti-correlated" with the solar radiation. The largest gain from the collector is in the Danish case obtained in March, and since the load in this season is diminishing, the temperature of the storage rises rapidly. This subsequently diminishes the collection efficiency of the collector, since for periods of the day the input temperature for the collector circuit is no longer lower than that of the storage. For this reason, little energy is collected during summer, and it is not until November that the increasing load necessitates drawing large amounts of energy from the storage, so that its temperature may decrease and the collection efficiency again increase. However, at that time of year the total solar radiation is again low, so that the energy added to the storage cannot make up for the

energy drawn from it, implying that the storage temperature remains below the limiting value of 45°C until the following March. Also, the losses of heat through the surface of the storage tank are not negligible during the summer months of high storage temperature. For example, in August practically all the collected energy goes into replacing energy lost from the storage surfaces.

One may think that the high storage temperatures during summer can be avoided if the storage volume is increased. This is indeed so, if the collector area is not very large, but on the other hand the storage temperature will also be below 45°C for a long time. If the collector area is very large, the summer storage temperatures will not diminish with certain amounts of increase in storage volume because the amounts of energy collected during the early summer months will just be larger (and the collection efficiency higher owing to the lower storage temperature). Later in the summer, the storage temperature will again be high and the efficiency low. In this case, the energy stored in the tank will last longer (because the tank volume is larger), but it will also take longer to fill the storage during early spring. As a result of these effects combined, the coverage (as a percentage of the net load) by solar energy is a very slowly varying function of storage volume, as shown below in Fig. 6.34.

On the other hand, Figure 6.32 has shown that moving closer to the Equator (from the Danish 56°N to Calabria's 48°N), it becomes possible to achieve full solar coverage with manageable water storage volumes.
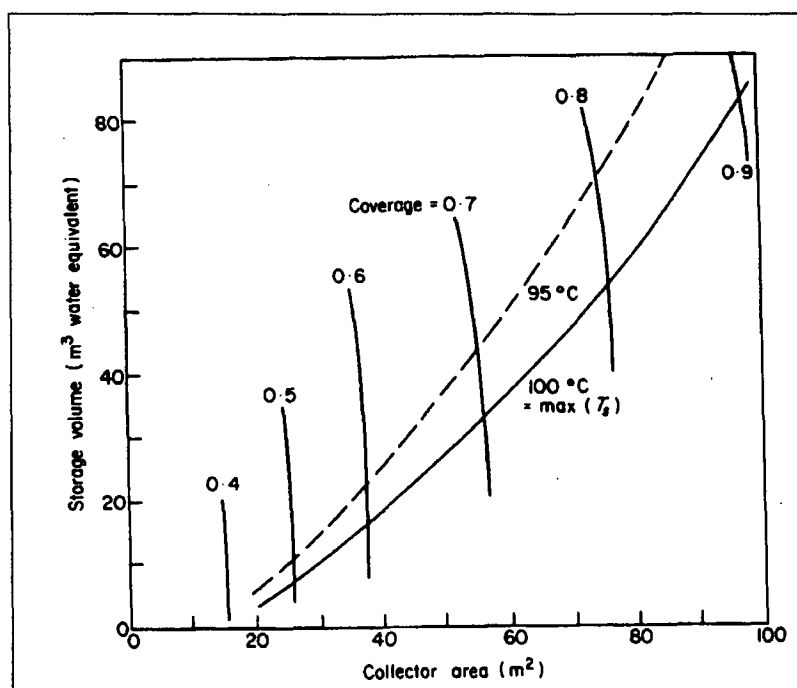

Figure 6.34. Fractional coverage of annual net load for Danish solar thermal system, as a function of collector area and storage volume (other parameters are as given in Table 6.5). Lines of maximum storage temperature reached over the year equal to or 5°C below the boiling point of water (under standard conditions) are also indicated (Sørensen, 1979).

For the Danish case (tilt angle 45° southward, selective absorber surface, one layer of glass cover), the annual coverage is in Fig. 6.34 given as function of collector surface and storage volume (other parameters, e.g. specifying storage insulation, remain as given in

Table 6.5). The coverage increases with increasing collector area, but more and more slowly. At a collector surface area of 15 m^2 the dependence is stronger than simple linearity, but from about 25 m^2 collector area the increase in coverage is less than linear, and complete coverage by solar energy is not reached by collector areas that would fit the south-facing part of the roof of the house.

The dependence on storage volume is extremely weak and the only reason for increasing the storage volume, when the collector area is increased, is to keep the maximum storage temperature below a certain value. This is required if the storage is based on water at standard pressure. In this case the maximum storage temperature during the year would have to be kept a little below the boiling point of water (say at 95°C), but for other types of storage medium, the temperature may be allowed to increase and the storage size may be quite modest, even for large collector areas.

The only way to improve the dependence of coverage on storage volume is to increase the insulation of the storage (or otherwise reduce the heat losses from the storage). An example of the improvement that can be obtained in this way is given in Figure 6.35. The obvious way to obtain such low heat losses is to build common storage facilities for several buildings. In areas where there have already been installed district heating lines, these may be used for distribution to and from a communal storage. The collectors would still be placed on the individual rooftops, but in this case it matters less if the orientation of some of the houses are unsuitable for solar panels. They can still be part of the common system, when collectors are optimally placed, implying that some buildings would become net heat exporters and other buildings net importers.

Also high-rise apartment buildings can be part of such a system, although often they have less suited areas for mounting collectors, relative to detached houses. They also typically have smaller heat demands, but not as significant as to offset the lack of surface areas exposed to solar radiation.

A common storage facility for a number of solar collector systems may offer several advantages. If the storage is in the form of heat capacity (e.g. a underground hot-water tank), then the heat losses through the insulation is reduced when a large number of individual tanks are replaced by a common tank of the same volume but having a surface area much smaller than the sum of the individual tank surface areas (smaller by the factor $N^{1/3}$ if N identical tanks are replaced by a common one of the same shape).

The disadvantage is the need to introduce heat transmission lines (if they are not already there), from the pipes of which additional heat losses will occur, depending on the average spacing between the houses or units sharing the storage facility.

Apart from directly reducing energy losses, the common storage system offers other advantages, such as providing heat for a single house while its collector system is malfunctioning or under repair, or as mentioned to allow some poorly oriented houses to take part in the common heat system. However, as always with centralised systems, there is also the risk of losing heat provision for all the houses simultaneously if the central system breaks down and repair involves disconnecting the services.

The performance of systems with common energy storage for an increasing number of house units, for fixed insulation thickness of the tank insulation ($U_s = 0.2$ Wm^{-2} °C^{-1}), is illustrated in Figs. 6.35, where the top abscissa units are the number of housing units with common storage (in the calculation assumed divided into two half-spheres, in order to simulate temperature stratification). Transmission losses are not included. It can be seen that using a common storage for 10 units corresponds approximately to doubling the storage insulation (bottom abscissa units), while a common storage for 100 units corresponds roughly to a four-fold increase in insulation thickness. There is seen to be marginally possible to supply 100% of the heat load even under the Danish conditions.
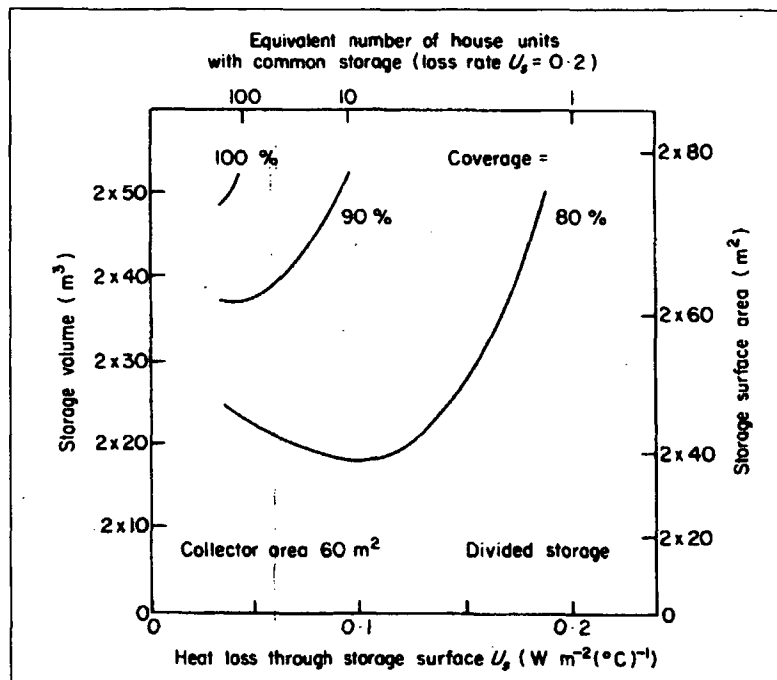
Figure 6.35. Percentage coverage of annual load for the Danish system, as function of the heat loss and storage volume. The storage is assumed to be spherical, and temperature stratification is simulated by allowing the upper and lower half-sphere to have different temperatures. The heat loss coefficient can be thought of as representing the number of houses sharing a common water storage container. The remaining parameters were in the simulation are fixed at the values given in Table 6.5 (Sørensen, 1979).

A general question to consider is whether dense building zones, such as apartment buildings, office buildings and some industrial buildings, and buildings used for commerce or public services, are suited for solar heating. Many of these buildings are placed, or can be placed, in such a way that solar collectors installed on roof and sides will become exposed under most conditions, despite shadow effects from other structures. The question is then, whether the area offered for collection purposes is sufficient to cover the heating loads of the individual building. If the loads are still taken as comprising only space heating and hot water, it may first be noted that the building surface to volume ratio is typically much more favourable than in one-family individual houses. With similar insulation standards, this implies that the hot water load will become relatively more important in an apartment building, assuming the same usage patterns as for the individual dwellings. This is an advantage in connection with a solar heating system, because the water need is approximately constant throughout the year, and not seasonally "anti-correlated" with the solar radiation like the space heating load.

One expects an even greater advantage for non-residential types of buildings, as mentioned above. They are generally characterised by being occupied only during day hours ("working hours"), and hence by an almost complete absence of heating requirements during the night hours, which are precisely the hours characterised by the highest heat losses from a fixed indoor temperature (i.e. the largest differences between a fixed indoor temperature and the ambient temperature outside). If night indoor temperatures are allowed

to drop (within proper limits, e.g. set by equipment that may be sensitive to excessive variations), the heating load may be greatly reduced on average.

---

1. Building heat losses

Loss rate through surface (except windows) 75 W °C^{-1}.

Loss rate through windows (no shutters) 40 W °C^{-1}.

Ventilation air 250 m^{3}h^{-1} from 16:00 to 08:00, 125 m^{3}h^{-1} from 08:00 to 16:00.

Minimum inlet temperature required at load, 45 °C.

Indoor temperature 21°C.

Hot water usage: 50 kg from 07:00 to 08:00, 25 kg h^{-1} from 16:00 to 24:00.

Required hot water temperature: 40 °C above an assumed input temperature of 5 °C.

2. Indirect heat gains

Persons: 300W from 00:00 to 07:00, 400 W from 07:00 to 09:00 and from 21:00 to 24:00,
· 500 W from 16:00 to 21:00, and 100 W from 09:00 to 16:00.

Equipment: 50 W from 00:00 to 07:00 and from 08:00 to 12:00, 550 W from 07:00 to 08:00 and from 16:00 to 17:00, 150 W from 12:00 to 16:00, 1050 W from 17:00 to 18:00, 650 W from 18:00 to 19:00, and 250 W from 19:00 to 24:00.

Lighting: 400 W from 07:30 to 08:30 and from 15:30 to 00:30, unless global solar radiation exceeds 50 Wm^{-2}, zero otherwise.

Gains from 20 m^2 vertically mounted windows, of which 15m^2 facing south, the rest north. Glazing: three layers of glass with refractive index 1.526, extinction coefficient times glass thickness (the product xL in (4.82)) 0.05. The absorptance $\alpha^{sw} = 0.85$ is used in (4.82) to specify the rooms behind the windows.

3. Flat-plate solar collector

Area 60 m^2, tilt angle 45°, azimuth 0° and geographical latitude 55–69°N. (Danish Reference Year).

Albedo of ground in front of collectors, 0.2.

Plate absorptance $\alpha^{sw} = 0.94$, emittance $\varepsilon^{lw} = 0.11$.

Cover system: one layer of glass (refractive index 1.526, xL in (4.82) equal to 0.05, emittance $\varepsilon^{lw} = 0.88$).

Heat capacity of collector: 1.4 + 0.7 times number of glass layers (Wh m^{-2} °C^{-1}).

Back loss coefficient (4.85): 0.2 W °C^{-1}m^{-2}.

Collector circuit flow rate times fluid heat capacity, $J_mC_p = 41.8$ W °C^{-1} per m^2 of collector area.

4. Storage facility

Capacity of heat storage given in terms of sensible heat storage in a container holding 40 m^3 of water.

Storage loss coefficient, 13.5 W °C^{-1} (relative to soil at 10°C).

Heat exchange rate between collector circuit and storage assumed to be practically perfect (100 W °C^{-1} per·m^2 of collector).

Table 6.5. Parameters used in simulation of a Danish solar heating system (Sørensen, 1979).

6.5 Short- and long-term storage system development

Solar thermal systems with short-term storage can be said to be fully developed, ranging from simply thermosyphon systems with a few hours worth of storage, used e.g. in Mediterranean holiday resort areas, to forced circulation systems with more substantial storage, used at lower latitudes for hot water and cold season heating, and at higher

latitudes mainly for hot water provision. The reason that low-efficiency natural circulation (thermosyphon) systems work in vacation areas is that such areas have a heat load peaking during summer. E.g. for islands such as Crete (Greece) or Cyprus, the population is typically 5-10 times higher during the summer holiday season than during winter. Thus, even simple systems aimed at satisfying the summer demand may in fact turn out to be sufficient year round.

At higher latitudes, currently typical systems with forced circulation and around 100 m^3 of water store per m^2 of collecting surface do well for summer hot water coverage. If the collectors are high quality (flat selective surface or better evacuated tube collectors), there is also some gain during spring and autumn, allowing coverage of part of hot water and space heating needs for well insulated houses, eventually incorporating some thermal mass storage. This assumes well-designed stores, possibly placed in each building, having optimally placed inlets and outlets and using temperature stratification. These systems are commercially successful in some countries and less in other countries, where they are 50-100% too expensive relative to current alternatives (oil and gas with environmental tax externalities, cf. Kuemmel et al. 1997). The lack of competitiveness even after several decades of development usually can be blamed on industry size (small companies without capital for long-term market development and therefore not achieving the associated price decline), on improper installation procedures (expensive general artisan installation rather than installation by specially trained solar system installers), or inappropriate financing and maintenance procedures (discouraging potential customers due to uncertainty of cost, both at installation and during operation).

Seasonal storage systems cannot be said to have reached commercial viability. However, a few R&D installations have proven the technical viability of some of the designs tried, although still being far from economic viability. Among these are some of the early installations in Sweden: A 10000 m^3 store excavated in rock and serving 55 semidetached one-family houses with a total of 2600 m^2 of flat-plate collectors (Margen, 1980), and a floating inverse cone store of 610 m^3 in Studsvik, having floating top insulation carrying 120 m^2 of concentrating solar collectors (Roseen and Perers, 1990). This system, shown in Figure 6.36, serves 500 m^2 of office space, and both systems have been operated since 1979.
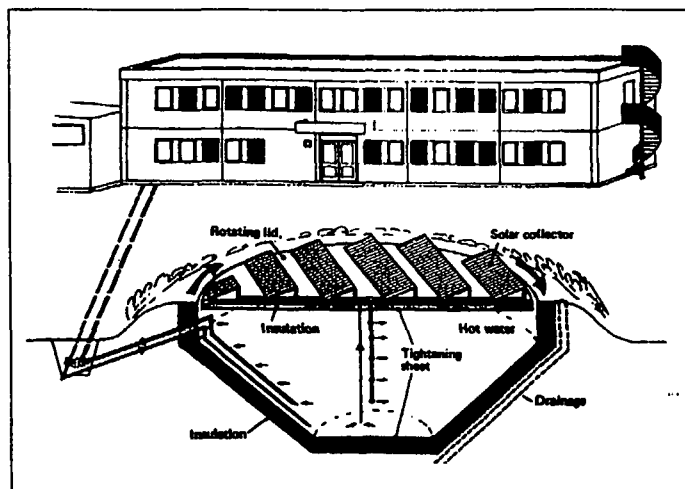

Figure 6.36. Layout of solar heating installation with seasonal storage in Studsvik (Roseen and Perers, 1980; Eriksson et al., 1989).

The temperature profiles for the Studsvik installation is shown in Figure 6.37. It is seen that the operating temperature is never above 70°C, and that temperature stratification in the store enables a gain in around 5°C for extracted heat, relative to the average temperature of the store (Jensen and Sørensen, 1984). The fact that heating loads in an office building is limited to day-time hours made it possible in this case to arrive at practically 100% heat coverage year round. More recent installations try to increase the working temperature, up to around 90°C, by adding insulation on all sides of the store. This is used for buffer stores connected to district heating systems (sizes of the order of 50000 m^3) and could also be the solution for large seasonal stores (Eriksson *et al.*, 1989). Systems such as the one in Calabria described above show that this is technically feasible, at least at mid-latitudes. Stratification of temperatures in the store has been investigated in several studies. It may improve the overall efficiency by some 20% (Hollands, 1989; Yoo et al., 1998; Alizadeh, 1999).
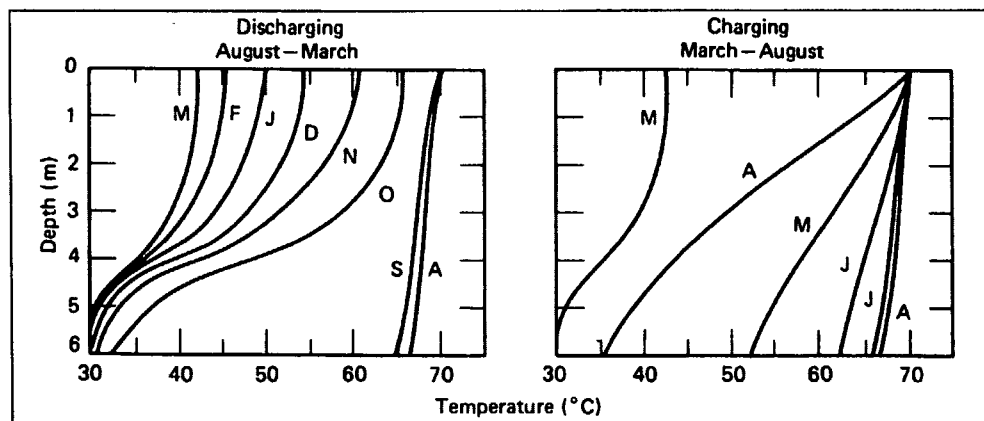

Figure 6.37. Monthly average temperatures in the Studsvik seasonal water store, during month of filling (right) and during months dominated by discharge (left) (Roseen, 1978; Jensen and Sørensen, 1984).

During most of the late 20th century, it was believed that viable seasonable storage systems for use with solar thermal systems would probably have to use technologies other than heat capacity storage. Foremost among these ideas were the use of phase-change or other chemical reactions, such as the absorption and release of crystal water by Na$_2$S (used in the Tepidus system, Bakken, 1981). A survey of the range of possibilities may be found in Sørensen (2000). Common for all these solutions is a system cost, which is 2-5 times that of current systems (without environmental externalities). This indicates the possibility of reaching economic viability, once technology and market developments have taken place. However, there are no systematic efforts at the moment to suggest that such development is going to take place.

6.6   Concluding remarks

Renewable energy options for thermal applications include combustion of biomass and use of thermal solar collectors. Combustion of biomass is in many cases more polluting than combustion of fossil fuels and is in a long-term sustainable view likely to be replaced by

conversion of biomass to high-quality types of energy (such as biofuels for the transportation sector). Solar thermal is an option that competes with photovoltaics for building roof and facade space. Because it provides low-quality energy, it is unlikely that central thermal plants will be found acceptable in areas with competition for land use.

It is characteristic of renewable energy conversion techniques, that the options that deliver high-quality energy such as fuels (from biomass) and electricity are abundant (photovoltaic panels and wind turbines in particular), and a future renewable energy system therefore will provide generous high-quality energy in good agreement with the energy use trends of increasing demands for high-quality energy. Still, the surplus of high-quality energy from renewable systems likely exceeds demand, implying that some will be used for lower quality uses such as mid-temperature process heat and low-temperature uses. As renewable energy will remain fairly expensive to harvest, it is clear that efforts should be made to use these energy sources efficiently, which in the case of lower-quality heat means using the heat pump principle to minimise the expenditure of high-quality energy for a given heat output.

Consider then the use of photovoltaic electricity to cover low-temperature heating needs. The efficiency of the solar-to-electricity-to-heat conversion route employing heat pump technology is fairly high: A heat pump is characterised by a coefficient of performance (COP) giving the ratio of low-quality heat output to high-quality energy input. Assuming 15% efficient solar cells and COP=3.33 heat pumps the total thermal efficiency is 50%. Thermal solar collectors may have a direct efficiency of 50-60%, but after the heat produced has been through a heat store, e.g. a community storage system, in order to satisfy demand when there is no solar radiation, the overall efficiency is much lower. Because most of the heating demand is at high latitudes, seasonal storage is required, with a turn-around efficiency of no more than of the order of 25%, at least if conventional heat-capacity storage is used. Thus the overall efficiency of the solar-to-heat-to-stored heat-to-useful heat is some four times lower than for the photovoltaic route. The low-temperature source for the heat pumps may be environmental heat from the ground or waterways, as air systems are inefficient at the high latitudes where most of the heat demand exist. Convenient techniques have been developed to inject ground pipelines for heat pump systems, without having to dig into the soil (Sørensen, 2000). Using solar electricity to cover heating needs thus seems the best solution. Only if the expected cost reductions assumed for photovoltaic systems turn out not to materialise, the solar thermal option might again seem more attractive.

References

Alizadeh, S. (1999). An experimental and numerical study of thermal stratification in a horizontal cylindrical solar storage tank. *Solar Energy*, **66**, pp. 409-42.

Bakken, K. (1981). System Tepidus, high capacity thermochemical storage/heat pump. In "Proc. Int. Conf. Energy Storage, Brighton", pp. 23-28. BHRA Fluid Engineering, Cranfield, UK.

Balcomb, J., Hestnes, A.-G., Hastings, S. (1996). IEA Solar Heating and Cooling Programme, Task 13: Strategies for solar energy houses. Chapter 1 in *Solar Energy Houses*. James and James, London.

Blarke, M. (1997). Marstal, Denmark - the World's largest solar thermal plant. In *World Directory of Renewable Energy Suppliers and Services 1997*. pp. 145-146. James and James, London

Dalenbäck, J. (1997). Evaluation of existing plants. In *Large-scale solar heating systems,* final report from EC project APAS/RENA CT 94-0057, Steinbeis TZ, Stuttgart.

Duffie, J. and Beckman, W. (1974). Solar energy thermal processes. Wiley, New York.

Eriksson, L., Zinko, H. and Perers, B. (1989). Design of a high temperature pit storage for seasonal storage. In "Proc. North Sun Conf. 1988", pp. 131-138. Swedish Council for Building Research, D2, Stockholm.

European Solar Industry Federation (1996). Sun in action: the solar thermal market, a strategic plan for action in Europe. EC Altener project report.

Fisch, M., Guigas, M. and Dalenbäck, J. (1998). A review of large-scale solar heating systems in Europe. *Solar Energy,* **63**, 355-366.

Hilmer, F., Vajen, K., Ratka, A., Ackermann, H. Fuhs, W. and Melsheimer, O. (1999). Numerical solution and validation of a dynamic model of solar collectors working with varying fluid flow rate. *Solar Energy,* **65**, pp. 305-321.

Hollands, K. (1989). Recent developments in low.flow, stratified-tank solar water heating systems. In "Proc. North Sun Conf. 1988", pp. 101-110. Swedish Council for Building Research, D2, Stockholm.

Jensen, J. and Sørensen, B. (1984) Fundamentals of Energy Storage, Wiley, New York.

Kasten, F. (1977). Solar Energy, **19**, 589-593.

Kuemmel, B., Nielsen, S. and Sørensen, B. (1997) Life-cycle analysis of energy systems. Roskilde University Press, Copenhagen.

Lamaris (1997). The European solar thermal market. In *World Directory of Renewable Energy Suppliers and Services 1997.* pp. 142-144. James and James, London

Leemans, R. and Cramer, W. (1998) IMAGE2 climate database, available at website http://www.pik-potsdam.de/public/climate

Margen, P. (1980). *Sunworld,* **4**, pp. 128-134.

Mathioulakis, E., Voropoulos, K. and Belissiotis, V. (1999). Assessment of uncertainty in solar collector modelling and tresting. *Solar Energy,* **66**, pp. 337-347.

NCEP/NCAR (1998) 40-year reanalysis project. Bull. Am. Met. Soc.; data available at website http://ingrid.ldgo.columbia.edu/sources under NOAA-NCEP-NCAR CDAS-1.

Nielsen, S. and Sørensen, B. (1996). Interregional power transmission: a component in planning for renewable energy technologies. In Proc. "Renewable Energy Conference, Cairo" (unpublished) and in *Int. J. Global Energy Issues,* **13**, No. 1-5 (2000; in press).

Oliveti, G, Arcuri, N. and Ruffolo, S. (1998). First experimental results from a prototype plant for the interseasonal storage of solar energy for the winter heating of buildings. *Solar Energy,* **62**, pp. 281-290.

Roseen, R. (1978). Central solar heating starion in Studsvik. AB Atomenergi Report ET-78/77. Studsvik, Sweden.

Roseen, R. and Perers, B. (1980). A solar heating plant in Studsvik. Design and first-year operation experience. Swedish Council for Building Research, Report D21, Stockholm.

Sørensen, B. (1976). Solar heat systems for use at high latitudes. In "Proc. UNESCO/WMO Solar Energy Symposium". WMO paper 477, Geneva.

Sørensen, B. (1979) Renewable Energy, Academic Press, London.

Sørensen, B. (1999) Long-term Scenarios for Global Energy Demand and Supply, Text 359 from IMFUFA, Roskilde University, Roskilde.

Sørensen, B. (2000) Renewable Enegy Second Edition, Academic Press, London (in press), see also information on website http://mmf.ruc.dk/energy

Thekaekara, M. (1976). Solar Energy, **18**, 309-325.

Yoo, H, Kim, C-J. and Kim, C. (1998). Approximate analytical solations for stratified thermal storage under variable inlet temperature. *Solar Energy,* **66**, pp. 47-56.

INTEGRATION OF PHOTOVOLTAIC CELLS INTO THE GLOBAL ENERGY SYSTEM

Bent Sørensen, professor of physics

Energy & Environment Group, Institute 2

Roskilde University, Bld. 02, Universitetsvej 1, DK-4000 Roskilde, Denmark

email: bes@ruc.dk, web: http://mmf.ruc.dk/energy

1. INTRODUCTION

Photovoltaic cells, also called solar cells, are devices that convert light into an electric current. Their present use is in a number of niche areas, from powering space vehicles and remote installations to powering small-scale consumer electronics. The cost of solar cells has dropped consistently over the last four decades, but is still very high compared to other bulk-power devices such as wind turbines (leaving apart the question of fossil or nuclear power plants, the cost of which include poorly known environmental externality costs). Therefore, solar cells compete in terrestrial uses only for rural electrification and telecommunication installations away from existing grids, and for special application, where ease of maintenance, dependability and the absence of emissions and noise are considered important. In addition, there has been and is currently being implemented several demonstration programmes of building integrated or centralised photovoltaic power, which signals the belief that increased volume of production, along with technological improvements, will bring the cost further down and eventually allow solar power to enter the area of mainstream applications.

The present chapter is aimed at describing the options for integration of photovoltaics into future energy systems. First, the current and emerging solar cell technologies of interest to scenario builders are briefly reviewed. The purpose is to demonstrate, that there is still many quite different solar technologies competing, and scope for more than marginal improvements of performance and

cost, which is a natural state of affairs for a technology that still needs to lower cost by a factor of 5-10. Second, the solar resource is assessed, as well as the potential power production on a geographical basis, taking into account constraints of land use and availability of surfaces suitable for building integration. Third, I present scenarios for integrating photovoltaic technologies together with other renewable energy technologies into a viable overall system capable of providing the power needed by future societies, with consideration of temporal and spatial requirements in different areas of the world. Finally, some concluding remarks are offered, dealing with the conditions needed and decisions having to be made in order to make such systems become realities.

2. PHOTOVOLTAIC TECHNOLOGIES

Below, the main types of currently considered solar cells are reviewed, with comments on module and system layouts. The basic physics of solar cells is e.g. described in [1].

2.1 Monocrystalline cells

Mono-crystalline cells are cells constructed from single crystals, usually in the form of ingots sliced into a number of cells. Refinements over the years have brought the cell efficiency for mono-crystalline silicon cells from a few percent up to about 25%. The light capture is improved through trapping structures that minimise reflection in directions not benefiting the collection area, and by back-side designs reflecting light rays back into the active areas. The doping degree is altered near electrodes, and a thin oxide layer further helps to prevent electrons reaching the surface rather than the electrode (this process being termed "passivation"). Further, top electrodes may be buried in order not to produce shadowing effects for the incoming light [2]. Simulation of the light trapping and electron transport processes in 1, 2 or 3 dimensions has helped in selecting the best geometry and degree of doping [3,4].

2.2 Multicrystalline cells

A newer technology for producing solar cells uses multicrystalline (some-times referred to as "polycrystalline") materials, instead of the single-crystal materials. Multicrystalline materials consist of small domains or grains of crystalline material, randomly oriented relative to each other. The crystal grains in multicrystalline materials sustain conductivity in the same way as single crystals do, but the transport of electrons across grain boundaries induces losses, reduces conductivity and thus makes the cells less efficient. On the other hand they can be produced by simpler methods than those needed for mono crystals, e.g. by evaporating suitable coatings onto a substrate. This field is in rapid development, as it is becoming possible to deposit only a few atomic layers onto a substrate, and with suitable techniques (such as using magnetic fields to align grains) it may soon be possible in this way to form near-monocrystalline layers without having to grow crystals.

Initially, it was believed that the additional losses at grain boundaries would necessarily make the efficiency of multicrystalline cells substantially lower than what is obtained by crystalline materials. However, the difference has recently narrowed, as a result of better understanding of the options for optimising performance of complex cell structures. One problem has been the damage inflicted upon multicrystalline cells by attempting to copy to them some of the efficiency-improving techniques that have worked well for monocrystalline cells (surface texturing, rear passivation by oxide layers). Yet, etching of inverted pyramids on the surface of multicrystalline cells has improved efficiency considerably and less damaging honeycomb texture patterns have brought the efficiency up to 20% [5]. This is a trend likely to complete the long-predicted change from expensive ingot-grown monocrystalline cell materials to deposition techniques for multicrystalline materials on suitable backings, much more suited for mass production and price reduction efforts. The advantages of thin-film multicrystalline solar cells over monocrystalline ones would seem to more than compensate for the remaining 5% efficiency difference.

2.3 Stacked cells

It is possible, instead of basing a solar cell on just a single p-n junction, to stack several identical or different cells on top of each other. The use of different cell materials aims at capturing a wider range of frequencies than possible with a single junction. In this case materials of different band gaps will be stacked. In the case of stacked identical cells, the aim is to be able to use low-quality material (e.g. the mentioned thinly sprayed crystalline cells in contrast to ingot-grown ones) and still get an acceptable overall efficiency by stacking several layers of low individual efficiency [6]. A broad maximum of efficiency over 15% has been achieved for a stacked cell structure with about six layers, using vapour deposition to deposit each layer and laser grooving to make room for electrodes. Module assembly is eased by using a design allowing automatic series connection. The dependence on the number of layers is weak for the optimum bulk doping concentration of about 10^{18} cm^{-3} and a total thickness of around 10 μm.

2.4 Amorphous cells

Amorphous semiconductor materials exhibit properties of significant interest for solar cell applications. While elemental amorphous silicon has a fairly uniform energy distribution of electron levels, composite materials have been constructed which exhibit a pronounced energy gap, i.e. an interval of energy essentially without any states, as in a crystal. Spear and Le Comber [7] first produced an amorphous material, which was later proved to be a silicon-hydrogen alloy. Doping (introduction of boron or phosphorus atoms) is possible, so that p- and n-type amorphous semiconductors can readily be made, and a certain amount of "engineering" of materials to exactly the desired properties with regard to gap structure, doping efficiency, conductivity, temperature sensitivity and structural stability (lifetime) can be performed.

Shortly after the discovery of amorphous solar cells, Japanese scientists succeeded in creating designs of such cells that were suited for industrial production [8] and soon found a market in

powering calculators and similar small-scale devices, where the cell cost was relatively unimportant. Band gaps in the range from 1.0 to 3.6 eV can be engineered with different silicon alloys (SiGe, Si, SiC), and such cells may be stacked to obtain a broader frequency acceptance. However, the simplest version has just one type of material: an intrinsic layer of an a-Si:H compound is the main area of light absorption, and adjacent p- and n-type layers ensure the transport to the electrodes, of which the front one is made of a transparent material. The whole structure is less than 1 μm thick and is deposited onto a plastic backing material.

Maximum efficiencies of around 13% have been demonstrated, but one problem has persisted: because the structure of the material is without order, bombardment with light quanta may push atoms around, and the material degrades with time. Current practice is to degrade commercial cells before they leave the factory, thereby decreasing the efficiency by some 20%, but in return obtaining reasonable stability over a 10-year period under average solar radiation conditions [9]. Several layers of p-, i- and n-layers may be stacked, and the highest efficiency is obtained by replacing the amorphous n-layers by a multicrystalline pure Si or silicon compound layer.

2.5 Other materials and other thin-film cells

Use of materials from the chemical groups III and V, such as GaAs, CdS and CdTe, instead of silicon allows better engineering of band gaps in crystalline solar cells to suit particular purposes, and brings forward new properties suitable for certain tasks (notably space applications and use in concentrating collectors). Important considerations in selecting materials include temperature dependence where crystalline silicon cell efficiency drops rather fast with the increasing temperature likely to prevail (despite possible active cooling) for cells operating at high levels of solar radiation (the efficiency drop is about 0.4% per °C for silicon [1]).

The GaAs bandgap of 1.43 eV is well suited for the solar spectrum, and with a tandem cell of GaAs plus $GaInP_2$ an efficiency of over 30% has been reached [10]. At the moment these cells are expensive and are mainly used in space. However, thin film versions may be developed as in the Si case, as they already have for CIS cells (copper-indium-diselenide). The highest efficiency obtained so far is about 17% for a Cu (In,Ga) Se_2 structure [11].

2.6 Organic solar cells

Suitable organic materials can trap sunlight and convert radiation into other forms of energy. It has been attempted to copy this process in various ways. Calvin [12] considered a double membrane that would separate the ionised reactants of a photo-excitation process,

$$A + \text{light quantum} \rightarrow A^* ; \qquad A^* + B \rightarrow A^+ + B^- .$$

In addition, a transport system is needed to get the ions to an electrode. No practical version of this idea has been produced. The same is the case for a concept aimed at both removing CO_2 from the atmosphere and at the same time producing methanol [13]. The absorption of solar radiation is used to fix atmospheric carbon dioxide to a ruthenium complex [Ru], which is then heated with water steam,

$$[Ru]CO_2 + 2H_2O + 713 \text{ kJ mol}^{-1} \rightarrow [Ru] + CH_3OH + \tfrac{1}{2}O_2$$

One scheme that has been realised is the attachment of a ruthenium complex as a dye to TiO_2, which may then transport electrons formed by photo-excitation in the Ru-complex to an electrode. The process is similar to the dye-excitation processes used in conventional photographic prints. The Ru-complex is restored by a redox process in an electrolyte joining the other electrode, with use of a platinum catalyst [14]. Because a monolayer of a dye such as [Ru] = cis-(NCS)2bis(4,4-dicarboxy-2,2-bipyridine)-Ru(II) will absorb less than 1% of in-coming solar radiation, it is proposed to attach the dye to a three-dimensional conglomerate of small (nanocrystalline) balls of TiO_2, in order to increase the overall cell efficiency to about 10%. It should still be possible for the TiO_2 balls to

transfer the electron to the electrode through a series of collisions, as laboratory experiments have actually confirmed.

2.7 Module construction

Individual cells based on monocrystalline materials have a linear size of typically 1 to 10 centimetres (limited by techniques for growing ingots of monocrystalline material). Multicrystalline cells formed by deposition of silicon onto a backing (usually glass) may have larger cell size, and for amorphous cells, there are essentially no limitations. Amorphous cells have been produced on rolls of flexible plastic backing materials, with widths of 1-2 m and rolls of any length. The same may also become possible for other thin film types, such as spray-deposited multicrystalline materials.

It is customary to assemble cells into modules by a mixture of parallel and series connections, so that the resulting voltages become suitable for standard electricity handling equipment, such as inverters transforming the DC currents into AC currents of grid specifications and quality. Alternatively, microprocessor inverters may be integrated into each module or even into each cell, in order to minimise transport losses. In recent years, specific inverters optimised for solar cell applications have been produced, with an inverter efficiency increase from 90% to some 98% [15].

The technology is then characterised by two main solar radiation conversion efficiencies: the efficiency of each cell and the efficiency of the module sold to the customer. The latter is currently about 5% lower than the former, notably because of phase mismatch between the individual cell current components, but this does not need to be so, and the difference between the two efficiencies is expected to diminish in the future.

2.8 Optical subsystem and concentrators

Optical manipulation of incoming solar radiation is in use for both concentrating and non-concentrating solar cells. In the latter case, it serves the purpose of reducing the reflection on the

surface to below a few per cent over the wavelength interval of interest for direct and scattered solar radiation [5]. The collection efficiency exceeds 90% for wavelengths between 0.4 and 1.05 μm, and exceeds 95% in the interval 0.65 to 1.03 μm.

For large-factor concentration of light onto a photovoltaic cell much smaller than the aperture of the concentrator, the principles used for thermal systems apply unchanged. Most concentrators are designed to focus the light onto a very small area, and thus tracking the Sun (in two directions) is essential, with the implications that scattered radiation largely cannot be used and that the expense and maintenance of non-stationary components have to be accepted.

One may think that abandoning very high concentration would allow the construction of concentrators capable of accepting light from most directions (including scattered light). However, this is not so easy. Devices that accept all angles have a concentration factor of unity (no concentration), and even if the acceptance angular interval is diminished to say 0-60°, which would be suitable because light from directions with a larger angle is anyway reduced by the incident cosine factor, only a very small concentration can be obtained (examples such as the design by Trombe are discussed in [16]).

2.9 Use of residual energy

Given that practical efficiencies of photovoltaic devices are in the range of 10-30%, it is natural to think of putting the remaining solar energy to work. This has first been achieved for amorphous cells, which have been integrated into window panes, such that at least a part of the energy not absorbed is passed through to the room behind the pane. Of course, conductors and other non-transparent features reduce the transmittance somewhat. The same should be possible for other thin-film photovoltaic materials, including the emerging multicrystalline silicon cells.

Another possibility, particularly for photovoltaic panels not serving as windows, is to convert the solar energy not giving rise to a current into heat (as some of it in actuality is already). One may

think of cooling the modules of cells by running pipes through their bottom side, carrying the heat away by some fluid. Again the energy available for this purpose is the incoming radiation energy minus the reflected and the converted part. Reflection from the back side of the semiconductor material, aimed at increasing the path length of the photons in the material, could be chosen to optimise the value of the combined heat and power production, rather than only the power production. For concentrator cells, active cooling is needed in any case, because of the temperature dependence of the characteristics of the photovoltaic process [17].

The maximum electrical efficiency of a photovoltaic device implied by semiconductor physics is about 40% (unless many different materials are used), and the possible associated heat gain is thus of a similar magnitude.

3. SOLAR RESOURCE AVAILABILITY

Recent work [18,19] employs a geographical information system (GIS) to map solar resources on the basis of satellite data (radiation at top of atmosphere, albedo, downward radiation at surface) and to match it with demand modelling on a habitat basis (population density, energy demand intensity). PV potential use is based on estimates of practical areas for collection use (building roof areas, suitably inclined and oriented surfaces) combined with land use data (important for central receiver fields). Local measurement data have been converted to the GIS grid employed. This is a novel approach compared to previous assessment, planning and scenario work in the photovoltaic field, which has traditionally been country based.

The solar radiation model is obtained by using data for solar radiation incident on a horizontal plane. One set of data is based on an analysis [20] of satellite measurements of radiation, albedo (reflectance) cloud cover and attenuation of radiation in the air. Another study collects many types of weather and climate data [21] and uses balance equations and a global circulation model

(horizontal resolution about 210 km and 28 vertical levels) to improve the consistency of data [22]. As no ground-based observations are used for solar radiation, this is entirely based on top-of-the atmosphere fluxes and various absorption, reflection and attenuation processes plus the balance requirements at the Earth's surface. The two sets of data give similar results for solar radiation. The balance equations (difference between upwards and downwards short- and long-wavelength radiation and heat fluxes) do suggest a too high albedo over oceans, but the land data that we are using appear to be reliable. Figure 1 shows the radiation on a horizontal plane at the Earth's surface for selected months of 1997 [21].

In order to calculate the solar radiation incident on inclined surfaces, such as the ones characterising most solar panel installations, one would ideally need hourly data for direct and scattered radiation (or equivalently for direct and total global radiation). One would then assume that the scattered radiation is uniform to calculate its value for differently inclined surfaces. For the direct part, ray calculations with the appropriate angles between the direction to the sun and the normal to the collector surface have to be performed hourly. Such calculations have been performed and compared with measurements on inclined surfaces at several major solar installations and some weather stations [1]. Here global data are needed and only monthly average radiation data are readily available (at least with data sizes suitable for the present type of investigation), so an approximate relation has to be invoked.

The aim is to estimate the radiation on a surface tilted towards either North or South by an angle approximately equal to the latitude (as this gives the optimum performance) from the horizontal surface solar radiation data available. No great accuracy is aimed at, because the actual solar panel installations in the 2050 scenario will be of two types:

(a): Building integrated panels that will anyway be influenced by the structures at hand: some solar panels will be mounted on vertical facades, others on roofs being either flat or tilted, typically

by angles 30°, 45° or 60°. In all cases the orientation may not be precisely towards South or North, although we estimate the resource as comprising only those buildings facing approximately correct and not being exposed to strong shadowing effects from other structures. The penalty of incorrect orientation and tilting angle is often modest and mostly influences the distribution of power on seasons [1].

(b): Centralised solar farms will generally be oriented in an optimum way, using total production maximising for panels not tracking the sun. However, the majority of locations suited for central photovoltaic installations will be the desert areas of Sahara, the Arabian Peninsula, the Gobi desert and Australian inland locations. As these are all fairly close to the Equator, there is modest seasonal variations in solar radiation, and the horizontal surface data are often quite representative.

Regarding the many unknown factors regarding the precise inclination of actual installations, the following simple approximation was adopted [18,19] (originating from an analysis of the Danish latitude 56°N data by [1]): The radiation on a latitude-inclined surface in January and July are noted to be very nearly equal to the horizontal radiation in October and April, whereas the horizontal surface data for January and July are lower and higher than the inclined surface measurements, respectively. It is therefore decided to use the October and April horizontal data as a proxy for January and July inclined surface radiation, and construct the April and October inclined surface values as simple averages of the January and July adopted values. Furthermore, this procedure, which works well for the Danish latitude, will be less inaccurate for low latitudes, because of the relative independence of seasons mentioned above, and we simply use it for all locations.

The horizontal surface data shown in Figure 1 have been checked against predictions of the European general circulation model HADCM2-SUL [23], and the 1997 monthly solar radiation values were found to be very similar.

In order to derive the actual energy extracted from solar cell panels, a fixed conversion efficiency of 15% is assumed, which is a fairly conservative estimate for year 2050 technology, considering that the current efficiency of the best mono-crystalline cells is above 20% and that of amorphous cells near 10%, with multicrystalline cells falling in between. The 2050 technology is likely to be thin-film technology, but not necessarily amorphous, as new techniques allow crystalline or multicrystalline material to be deposited on substrates without the complicated process of ingot growth and cutting. The efficiency of such cells is currently fairly low, but as they are much less expensive than crystalline cells, they may be stacked in several layers and thereby still reach the efficiency envisaged here [6].

Finally, the availability of sites is estimated, for mounting solar cell panels either in a decentralised fashion or centrally in major energy parks: The decentralised potential is based on availability of suitably inclined, shadow-free surfaces. It is assumed that the area of suitably oriented surfaces that may be used for building-integrated PV energy collection is 1% of the urban horizontal land area plus 0.01% of the cropland area. The latter reflects the density of farmhouses in relation to agricultural plot sizes and is based on European estimates, roughly assuming that 25% of rural buildings may install solar panels. The potential PV production is thus taken as 15% of radiation times the fraction of the above two area types and the stated percentage for each. A final factor of 0.75 is applied in order to account for transmission and storage cycle losses, assuming about 5% transmission losses and that roughly half the energy goes through a storage facility of 60% round-trip efficiency (e.g. reversible fuel cells). The flow of energy reduced by all these

factors represents the energy delivered to the end-use customers in the form of electricity. It is shown in Figure 2 for each season, with regional sums given in Table 1.

Table 1. Regional averages and sums of solar energy-supply related quantities [18].

Region (see below)	1	2	3	4	5	6	Total	unit
Region area	20.1	15.4	28.3	26.3	20.1	30.9	141	M km^2
Urban area fraction	0.0063	0.0133	0.0096	0.0178	0.0290	0.0122	0.0147	
Marginal land fract.	0.1155	0.2166	0.1239	0.0999	0.3038	0.4058	0.2109	
Decentralised PV potential, January	38.9	40.5	71.3	146	164	109	570	GW
Decentralised PV potential, July	60.2	66.6	118	141	217	122	724	GW
Decentralised PV potential, ann. Av.	49.5	53.5	94.5	143	190	115	647	GW
Centralised PV potential, January	2220	7310	6680	4500	7910	18200	46900	GW
Centralised PV potential, July	3870	5990	9460	3980	11500	22700	57500	GW
Centralised PV potential, annual av.	3040	6650	8070	4240	9690	20500	52200	GW

Region 1: United States, Canada. Region 2: Western Europe, Japan, Australia. Region 3: Eastern Europe, Former Soviet, Middle East. Region 4: Latin America, SE Asian high-growth countries. Region 5: China, rest of Asia. Region 6: Africa.

For centralised PV, the estimated potential is based upon 1% of all rangeland plus 5% of all marginal land (deserts and scrubland), again times 15% of the incoming radiation and times 0.75 to account for transmission and storage losses. As shown in Figure 3 and Table 1, this is a huge amount of energy, and it shows that such centralised PV installations can theoretically cover many times the demand envisaged over the next centuries. Setting aside 1% of rangeland would imply an insignificant reduction in other uses of the land, even if this would rather be a small number of large plants. The same is true for desert and marginal land, where only the 5% most suited need to be invoked, which in reality might be 10% for the entire installation (including frames, access roads), of which the solar panels is only part. Because of the huge area of e.g. the Sahara desert this would suffice to supply more than the entire world need for energy. This would require the availability of intercontinental transmission, which may be quite realistic in the future, e.g. by use of superconducting trunk lines [24].

4. INTEGRATION OF PHOTOVOLTAICS INTO ENERGY SYSTEMS

In a project performed for the Danish Energy Agency [18], four global energy supply scenarios with zero greenhouse gas emissions have been constructed, based upon a common energy supply scenario. The supply scenario is constructed by a bottom-up approach, considering basic and secondary needs, development of social organisation and activities, region by region, and finally considering population growth and settlement patterns to the scenario year, 2050. The efficiency of energy conversions is assumed by 2050 to average the best efficiency in or close to the market today. Efficiency improvement is here meant to include the introduction of new technology to perform a task in a way different from the one used earlier, as well as straight improvements in the energy efficiency of a given piece of technology.

The supply scenarios comprise use of fossil fuels without carbon dioxide emissions to the atmosphere, using nuclear conversion techniques without risk of catastrophic accidents or proliferation of nuclear material, and renewable energy sources either in a purely decentralised mode, or with inclusion of some windfarms, central solar collector fields, and energy crops (although the need for such "centralised" facilities is far lower that the resources available). Here only the renewable energy scenarios will be discussed. Photovoltaic devices deliver about 20% and 30% of the total supply assumed in the two scenarios.

4.1 Energy end use

Demand scenarios for the 21st century found in literature are based either on extrapolation ("business-as-usual" scenarios) or on technically feasible, normative assumptions about the development of societies. In a greenhouse warming mitigation context, the interesting demand scenarios are those which aim at reducing emissions at a lower cost than that of supply-side measures (fuel shifts or transition to energy sources not emitting greenhouse gases). Studies have identified a number of measures not undertaken although they have no significant cost [25,26]. The

reason is inertia or opposition to "reductions" in energy use, seen as negative in the context of economic growth. As a result, measures at the supply side have been financed, that entail a higher cost per energy unit than that of suitable demand-side measures. One aim of greenhouse policies could be to change this attitude, e.g. by legislative means (such as building codes, standards for appliances, cars etc.) or by taxation (differential tax on cars and other equipment according to energy efficiency). Both types of policy means are in use in a few countries.

As an example of a demand scenario placing emphasis on demand-side measures, a bottom-up analysis based upon a vision of future global societies with high levels of prosperity will be discussed [18]. It will be underlying the global supply scenarios to be further discussed in section 4.2. The assumption is, that by the mid 21st century, the average technology in use will equal the best current technology, with respect to energy efficiency. This is compounded with increasing population (using middle scenario of UN forecasts [27]), increasing urbanisation (according to UN [28], and increased per capita activity level by an average factor 2.7 for energy use. The GNP activity growth factor will be larger due to the de-coupling of economic and energy growth, and the distribution between regions will not be even (because a larger growth rate is assumed for the presently poor regions).

Figure 4 shows the total energy delivered to the end-users in the 2050 scenario, including energy for space conditioning, process heat, stationary mechanical energy, electric energy, energy for transportation and energy in food, for all sectors of society. The average and totals for different regions are shown in Table 2, for each major energy type. The average energy demand is 0.9 W/cap. or three times the amount made useful at the end-user today. The energy made useful at the end-user today is only about 12% of the primary energy, and the challenge is to increase this fraction is the future [18].

Table 2. Energy delivered to end-user in 2050 scenario (from [18,19]). The six regions were defined in the footnote to Table-1.

Regions: / Energy quality:	1.	2.	3.	4.	5.	6.	Average / Total
Food based on animals	30	30	30	25	25	20	**23 %**
	45	45	45	37	37	25	**36 W/cap.**
	17	24	47	52	148	51	**339 GW**
Food based on grain & vegetables	70	70	70	75	75	80	**77 %**
	119	119	119	128	128	114	**123 W/cap.**
	45	63	124	177	506	232	**1148 GW**
Gross transportation energy	359	299	140	201	99	30	**125 W/cap.**
	136	158	146	277	392	61	**1170 GW**
Heat pump input for low-T heat and cooling	103	110	87	43	80	22	**65 W/cap.**
	39	58	90	60	318	45	**610 GW**
Environmental heat	240	256	203	100	186	51	**151 W/cap.**
	91	135	210	140	741	105	**1421 GW**
Direct electric and all other energy	420	424	245	288	283	47	**240 W/cap.**
	153	224	255	398	1116	96	**2242 GW**
Total delivered energy*	**1272**	**1252**	**838**	**800**	**814**	**290**	**742W/cap.**
	482	**661**	**871**	**1104**	**3225**	**591**	**6934 GW**
Population 2050	379	528	1040	1380	3960	2040	**9340 millions**

* Including heat drawn from the environment by heat pumps.

In terms of full satisfaction of all primary and secondary human goals, the demand scenario assumes that for regions 1 and 2 of Table 2, there is nearly 100% goal satisfaction, for regions 3-5 some 2/3 of full goal satisfaction, and for region 6 a satisfaction level of 1/5. These levels are significantly higher than the ones characterising regions 3-6 at present, as the detailed analysis of Sørensen [18] shows.

4.2. Global scenarios

A number of issues speak against merely optimising energy supply systems on a national or regional basis. These have to do with the cost and supply security implications of creating for some countries a dependence on resources that have to be imported from far away, but also with the desirability of preserving levels of international trade to which the economy of the currently exporting countries have become dependent.

In this chapter, different scenarios for future energy supply systems addressing the greenhouse warming issue are analysed with respect to their requirements for energy transmission and energy trade, with emphasis on whether the problem is local, regional or global.

The renewable energy resources are fairly evenly accessible, although there are distinct variations with latitude (solar radiation, cf. section 3) and absence of obstacles (wind power). For biomass resources, limiting factors include solar radiation, nutrients, water and soil quality. Adding the other renewable resources to those of solar radiation discussed in section 3, one obtains a total estimate of practical exploitable resources as shown in Figure 5.

The global scenarios for the mid-21st century discussed in [18] includes two renewable energy scenarios, which may be characterised as follows:

(A). *The decentralised renewable energy scenario*, based upon building-integrated solar systems and dispersed installations for utilising wind and biomass energy, the latter being based on integrated production of food, energy and bio-feedstock for industry.

(B) *The centralised renewable energy scenario*, placing additional solar collectors or wind turbines in areas of non-arable land, or off-shore in large farms. The scenario includes a cautious use of biomass plantations placed on land where competition with food production is considered minimal.

51

Figures 6 and 7 show the distribution of mismatch between supply and demand for the two scenarios. For both renewable energy scenarios, there are more surplus areas than deficit areas, and even in densely populated areas such as India or China, there are areas of surplus. The largest deficits are of course found in highly urban areas, where high-rise buildings make the surfaces suitable for solar collectors small compared with the demand, and where wind power and biomass production is not possible. In most cases, this implies a need only for local transport or transmission of energy, from cultivated country areas or marginal land to the cities or particularly population- or energy-intensive regions, usually of modest dimensions.

Upon closer inspection of the forms of energy required, it is seen that even for the projected population increase, average food supply is adequate in all parts of the world, leading only to the well-known need for land to city transfer, also for countries such as India and China. This is due to the scenario assumptions on improved agricultural techniques, consistent with assumptions of technological and economic growth in all parts of the world, and despite the slight decrease in yields implied by an assumed high proportion of ecologically grown food. For (bio-)fuels to be used in the transportation sector, there is a significant deficit in most of Europe, the Middle East and India, to be matched with surpluses in China, South-East Asia, Northern countries of South America and Northern countries of Asia, Europe and North America. This implies that biofuels have to be traded internationally, which is feasible as they can be transported much like oil.

For electricity, there are strong deficits in urban areas and in much of Central Europe, India and Eastern China, whereas surpluses occur in the rest of the world and for the decentralised renewable energy scenario particularly in South America. This makes the required trade in the decentralised scenario nearly impossible, unless some intercontinental electricity transmission technologies emerge. Transformation of surplus electricity to portable fuels would solve the problem, but there are barely enough decentralised resources to allow for the losses. By contrast, the

centralised renewable energy scenario has additional resources from agricultural and marginal land, making trade in the form of biofuels or electricity for more modest transmission distances capable of graciously solving the problem.

Table 3. Assumed energy supply (after storage conversion cycles and transmission but before interregional imports/exports) in centralised 2050 scenario, and corresponding supply-demand balances. The term "other energy" comprises all energy except energy in food and energy used for transportation. Source: [18].

Region (cf. Table 1)	1	2	3	4	5	6	Total	unit
Total food balance (as Table 10)	151	144	107	283	-23	-167	**493**	GW
Total biofuels used	250	190	300	640	327	192	**1899**	GW
Of which decentralised biofuels	250	166	236	640	295	192	**1779**	GW
Balance: total biofuels minus use for transportation	136	158	146	277	392	61	**1170**	GW
Hydro power	80	70	50	120	110	10	**440**	GW
Decentralised solar power	27	50	67	109	189	23	**465**	GW
Centralised solar power	40	20	114	19	400	100	**693**	GW
Decentralised wind power	20	37	80	100	100	10	**347**	GW
On-shore wind parks	12	10	20	38	46	0	**126**	GW
Off-shore wind power	0	40	0	0	13	0	**53**	GW
Balance: other energy, ann.av.	100	-63	139	288	-660	217	**22**	GW
Balance: other energy, Jan.	74	-120	169	306	-890	214	**-250**	GW
Balance: other energy, April	87	-51	72	243	-710	200	**-160**	GW
Balance: other energy, July	129	-17	180	352	-410	233	**461**	GW
Balance: other energy, Oct.	110	-64	129	252	-610	220	**35**	GW

Table 3 shows the regional totals of energy balances, with an indication of seasonal changes. It is seen that trade and transmission requirements vary from season to season, with quite large differences involved. The overall layout of the energy system is illustrated in Figure 8, for the centralised scenario, which has the highest share of photovoltaic, due to a modest addition of desert-located central solar power plants.

5. DISCUSSION AND CONCLUSIONS

For the scenarios based entirely on renewable energy flows of fairly low energy density, it is found that the decentralised scenario works well in some regions but on a global average basis (with

the restrictions posed by renewable resources available locally and consistent with the decentralisation paradigm), it barely matches the demand of the 2050 population with the assumed massively improved living standards. This implies that the scenario requires import of energy by countries such as e.g. India, and as surpluses exist mainly in South America and is dominantly in the form of electricity, the transfer will be difficult, and seemingly in contradiction with the "local self-sufficiency" idea behind the decentralised scenario.

By contrast, the scenario adding a certain amount of centrally produced renewable energy exhibits supply in generous excess of demand, and trade of energy between regions will allow the system to be very robust against changes in assumptions on demand development and area use. For example, desert regions in North Africa and the Middle East can export photovoltaic electric power to Europe and thereby create a basis for continued economic development without resort to oil.

While the positive economic implications of adopting the energy demand scenario with high emphasis on energy efficiency is evident, the economic aspects of the supply scenarios cannot be stated with certainty. The renewable energy technologies comprise hydro and wind power, which are largely economic today, biofuel technologies currently about two times more expensive than the current sources, and photovoltaic technologies currently more than ten times more expensive than conventional coal-fired power supply. Even considering externality costs, it is therefore clear that a cost reduction is needed, and projections suggest that such a cost reduction for photovoltaic power is indeed possible and forthcoming with continued market development support.

The more detailed discussion in [18] implies that the paradigm of extreme decentralisation (local or even individual control over energy supply) is not stable (e.g. towards variability between years of renewable resources) and that it requires international trade and transmission of energy of a size difficult to reconcile with the local self-sufficiency idea. The conclusion of this is that only the centralised renewable energy scenario offers a feasible sustainable energy supply system for the

long-term future, and that it is indeed very likely to become feasible in the near future, adding a modest amount of centralised wind and photovoltaic energy (wind-farms on-shore and off-shore, solar cell farms), plus a modest amount of biomass crops grown for biofuels, to the decentralised renewable energy systems. It is therefore imperative, that policy measures (such as liberalisation of electricity trade) do not obstruct this development.

6. REFERENCES

[1] Sørensen, B. 2000. *Renewable Energy*. Academic Press, London, 2nd edition, ca. 900 pp.

[2] Green, M. 1992. Crystalline and polycrystalline silicon solar cells. pp. 337-360 in *Renewable energy sources for fuels and electricity* (Johansson et al., eds.), Island Press, Washington

[3] Basore, P. 1991. PC1D v.3 Manual and User Guide. Report 0516/rev. UC-274. Sandia National Laboratory, Albuquerque.

[4] Sørensen, B. 1994. Model optimization of photovoltaic cells. *Solar Energy Materials and Solar Cells*, 34, 133-140.

[5] Zhao, J., Wang, A. and Green, M. 1998. 19.8% efficient multicrystalline silicon solar cells with "honeycomb" textured front surface, pp. 1681-1684 in *Proc. 2nd World Conf. on PV Solar Energy Conversion* (Vienna), JRC EUR 18656 EN, Ispra.

[6] Wenham, S., Green, M., Edminston, S., Campbell, P., Koschier, L., Honsberg, C., Sproul, A., Thorpe, D., Shi, Z. and Heiser, G. 1995. Limits to efficiency if silicon multilayer thin film solar cells, pp. 1234-1241 in *1994 First World Conf. on Photovoltaic Energy Conversion* (Kona), IEEE.

[7] Spear, W. and Le Comber, P. 1975. *Solid State Commun.* 17, 1193–1196.

[8] Hamakawa, Y., Tawada, Y. and Okamoto, H. 1981. *Int. J. Solar Energy*, 1, 125.

[9] Sakai, H. 1993. Status of amorphous silicon solar cell technology in Japan, pp. 169-172 in *Technical Digest of 7th Int. PV Science and Engineering Conf.* Nagoya Institute of Technology.

[10] Deb, S. 1998. Recent developments in high efficiency photovoltaic cells. *Renewable Energy*, 15, 467-472.

[11] Tuttle, J., Ward, J., Duda, A., Berens, A., Contreras, M., Ramanathan, K., Tennant, A., Keane, J., Cole, E., Emery, K. and Noufi, R. 1996. The performance of Cu(In,Ga)Se2-based solar cells in conventional and concentrator applications. In *Proc. Material Research Society Symposium*, 426, 143.

[12] Calvin, M. 1974. *Science*, 184, 375 – 381.

[13] Jensen, J. and Sørensen, B. 1984. *Fundamentals of energy storage*, Wiley, New York, 345 pp.

[14] O'Regan, B. and Grätzel, M. 1991. *Nature*, 353, 737.

[15] IEA 1999. *Photovoltaic power systems in selected IEA member countries*. 3rd survey report of the Power Systems Programme Task 1, International Energy Agency, Paris.

[16] Meinel, A. and Meinel, M. 1976. *Applied Solar Energy*. Addison-Wesley, Reading

[17] Wysocki, J. and Rappaport, P. 1960. *J. Appl. Phys.* 31, 571–578.

[18] Sørensen, B., 1999. Long-term scenarios for global energy demand and supply. *IMFUFA Texts 359.* Roskilde University, 212 pp.

[19] Sørensen, B. and Meibom, P., 1999. A global renewable energy scenario. *International Journal of Global Energy Issues* (forthcoming 1999).

[20] Pinker, R. and Laszlo, I., 1992. Modelling surface solar irradiance for satellite applications on a global scale. *J. Applied Meteorology* 31: 194-211.

[21] NCEP/NCAR, 1998. 40-year reanalysis project: Bulletin of the American Meteorological Society: data available at the website http://ingrid.ldgo.columbia.edu/sources in the catalogue of NOAA NCEP-NCAR CDAS-1 data sets.

[22] Kalney, E. et al., 1996. The NCEP/NCAR 40-year reanalysis project. Bulletin of the American Meteorological Society: available at the website quoted in [3].

[23] Mitchell, J. and Johns, T., 1997. On modification of global warming by sulphate aerosols, *Journal of Climate*, 10: 245-267. Model output (12 months by 240 years) available at IPCC Data Distribution (1998) website http://www.dkrz.de/ipcc/ddc/html/gfdlrun2.html

[24] Nielsen, S. and Sørensen, B., 1999. Interregional power transmission. *International Journal of Global Energy Issues* (forthcoming).

[25] Sørensen, B. 1982. Energy choices: Optimal path between efficiency and cost. pp. 279-286 in *Energy, resources and environment* (S. Yuan, ed.), Pergamon Press, New York.

[26] Sørensen, B. 1991. Energy conservation and efficiency measures in other countries. Australian Department of the arts, sport, the environment, tourism and territories, *Greenhouse Studies No. 8*. Commonwealth of Australia, Canberra.

[27] UN 1996. Populations 1989, 2015, 2050. United Nations Population Division and UNDP, Washington.

[28] UN 1997. Urban and rural population estimates and projections as revised in 1994. United Nations Population Division and UNDP, Washington.

FIGURE CAPTIONS:

Figure 1 (a): April 1997 average solar radiation on horizontal surface (above, downward energy flux at Earth's surface, W/m^2). *(b):* July 1997 average solar radiation on horizontal surface (below, downward energy flux at Earth's surface, W/m^2) Based on [1,18] using data from [21].

Figure 2 (a): January potential power production from building-integrated solar cells, with transmission and storage cycle losses subtracted (W/m^2, above). *(b):* April and October potential power production from building-integrated solar cells, with transmission and storage cycle losses subtracted (plain average of January and July values; W/m^2, below). *(c)*. July potential power production from building-integrated solar cells, with transmission and storage cycle losses subtracted (W/m2, above).Based on [18].

Figure 3. Potential annual average power production from centralised photovoltaic plants on marginal land, with transmission and storage cycle losses subtracted. Seasonal variations are modest (W/m^2; scale is linear in contrast to that of Fig. 2). Based on [18].

Figure 4. Total energy directly delivered to consumer in 2050 scenario (including environmental heat and the food, transportation and electricity etc. columns of Table 2). The scale of average energy flow in watts per square metre of land area is given to the right (from [18]).

Figure 5. Estimated total renewable energy resources, taking into account land restrictions due to alternative uses and for environmental reasons, as well as conversion losses. The sources include solar photovoltaic, wind, hydro, all for electricity, and biomass for fuels and food, given in units of energy flow (watts per square metre, scale to the right). From [18], where details of the individual resource estimates can also be found.
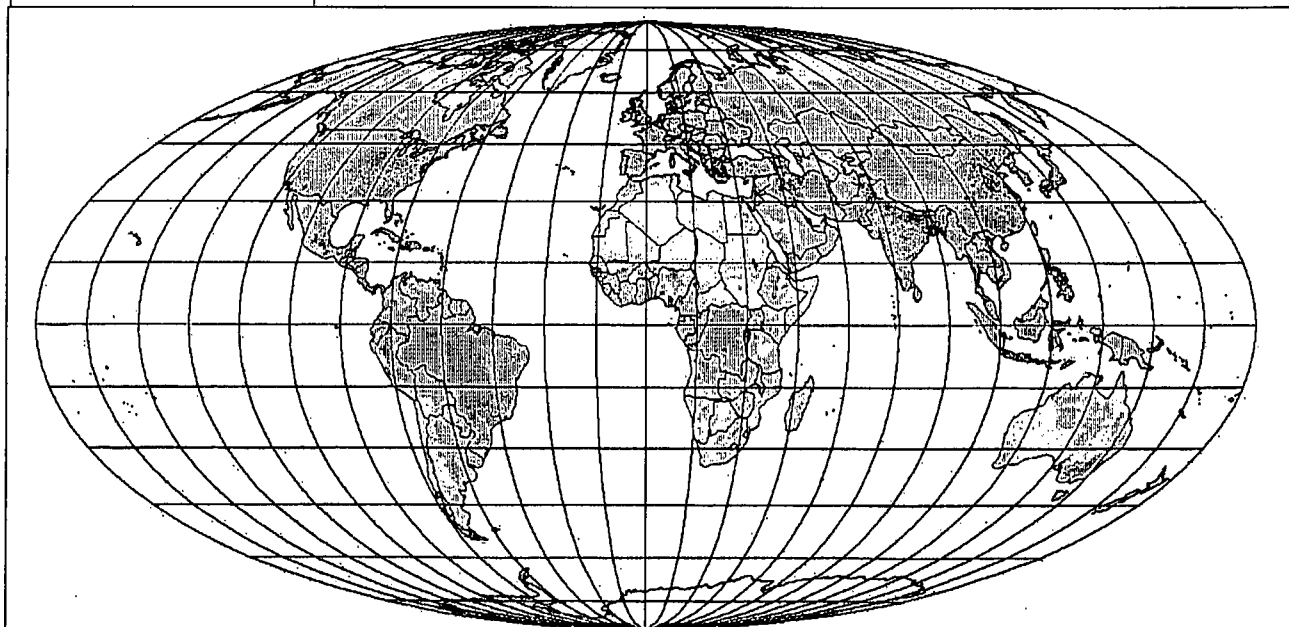
Figure 6. Difference between supply and demand, for the decentralised renewable energy 2050 scenario, using only building-integrated solar cells and farm-attached wind turbines, together with pesticide-free agriculture and bio-energy production only from agricultural and forestry residues, plus existing hydro power. The delivered energy supply comprises food, electricity and biofuels for stationary and transportation uses. Scale in W/m^2 is given to the left (from [18]).

Figure 7. Difference between supply and demand, for the centralised renewable energy 2050 scenario, using building-integrated and centralised solar cells on marginal land, wind turbines near farms and in parks on marginal land or off-shore, together with pesticide-free agriculture and bio-energy production from residues and a limited number of energy-crops or energy-forests, plus hydro power in place or under construction. The delivered energy supply comprises food, electricity and biofuels for stationary and transportation uses. Scale in W/m^2 is given to the left (from [18]).
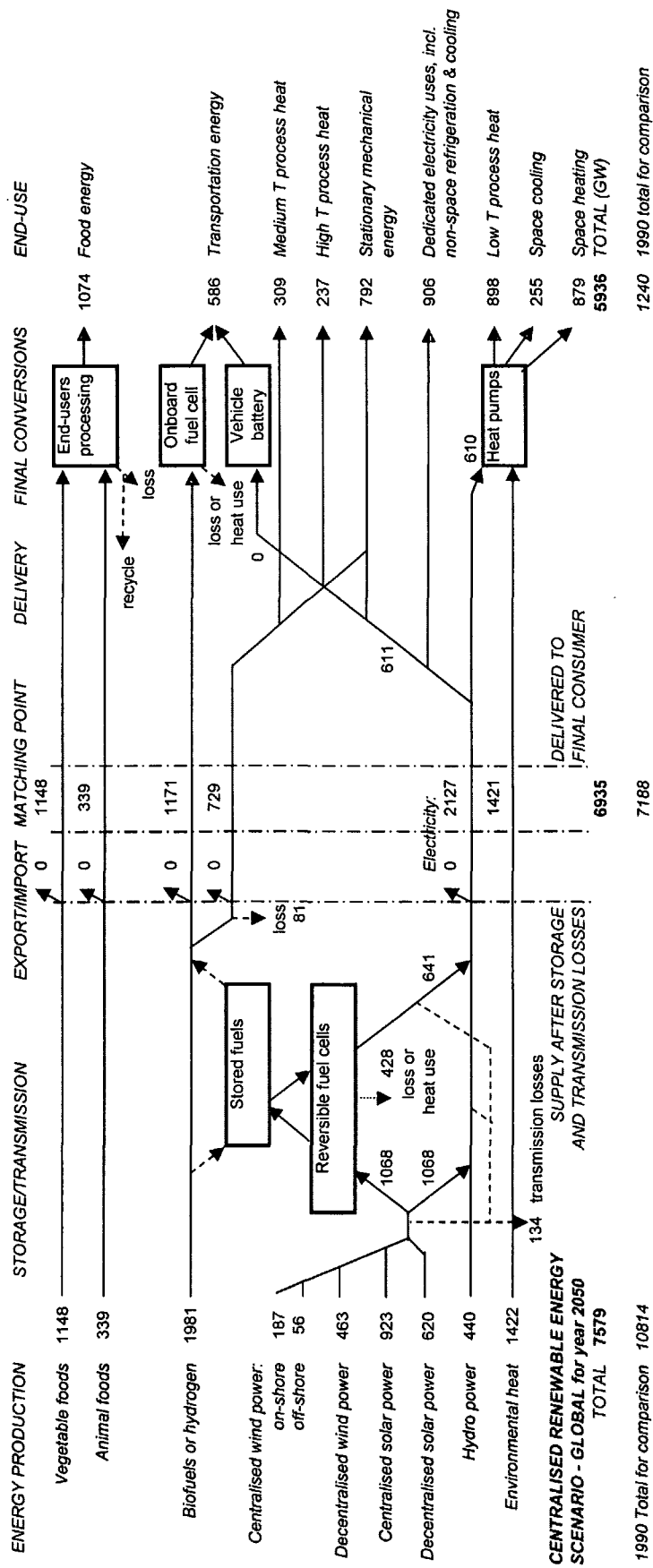
Figure 8. Overview of centralised 2050 renewable energy scenario (energy flows in GW or GWy/y). From [30].
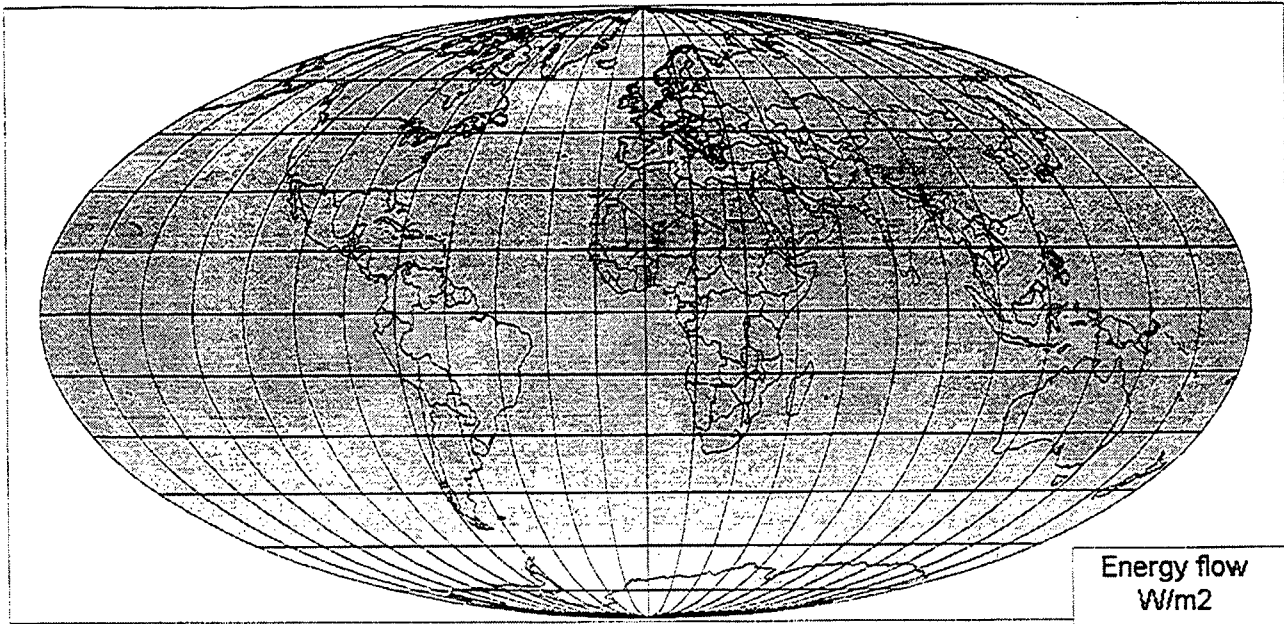
Figure 1a. April 1997 average solar radiation on horizontal surface (above, downward energy flux at Earth's surface, W/m^2)

Figure 1b. July 1997 average solar radiation on horizontal surface (below, downward energy flux at Earth's surface, W/m^2)

(based on [1, 18] using data from [21]).

Energy flow W/m2

440 to 480
400 to 440
360 to 400
320 to 360
280 to 320
240 to 280
200 to 240
160 to 200
120 to 160
80 to 120
40 to 80
0 to 40
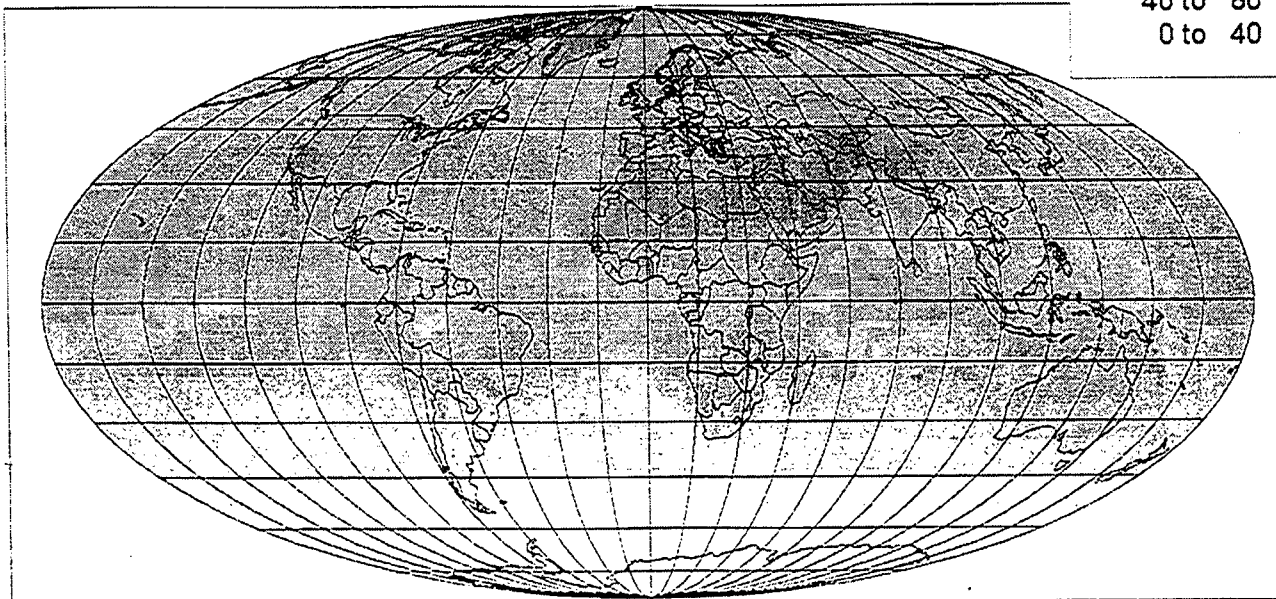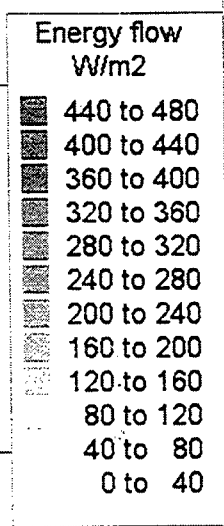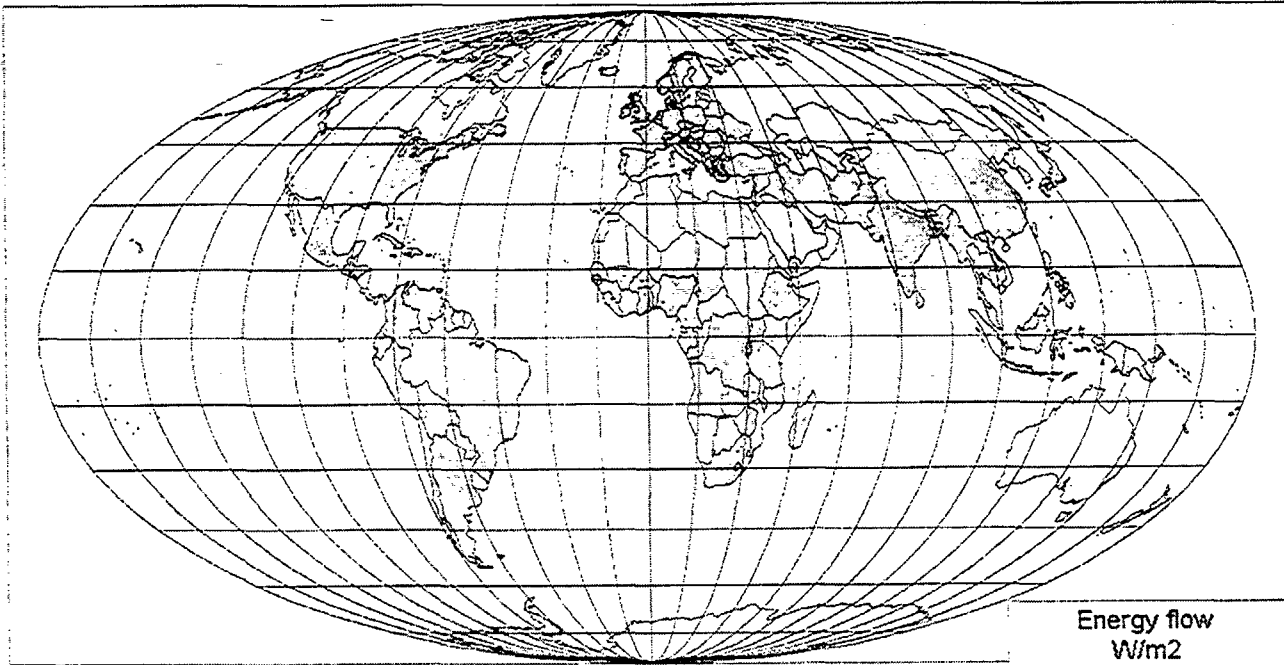
Figure 2a. January potential power production from building-integrated solar cells, with transmission and storage cycle losses subtracted (W/m², above).

Figure 2b. April and October potential power production from building-integrated solar cells, with transmission and storage cycle losses subtracted (plain average of January and July values; W/m², below).

(based on [18]).
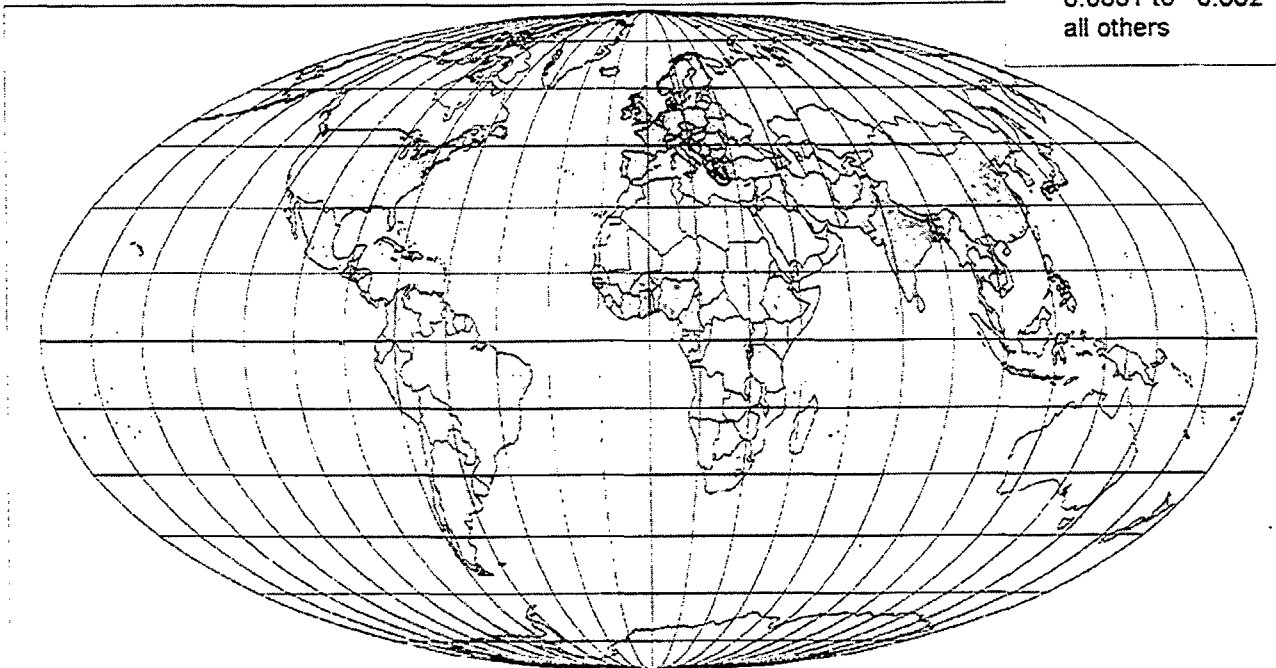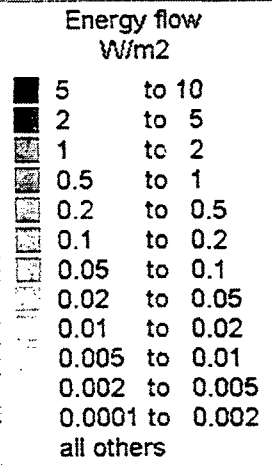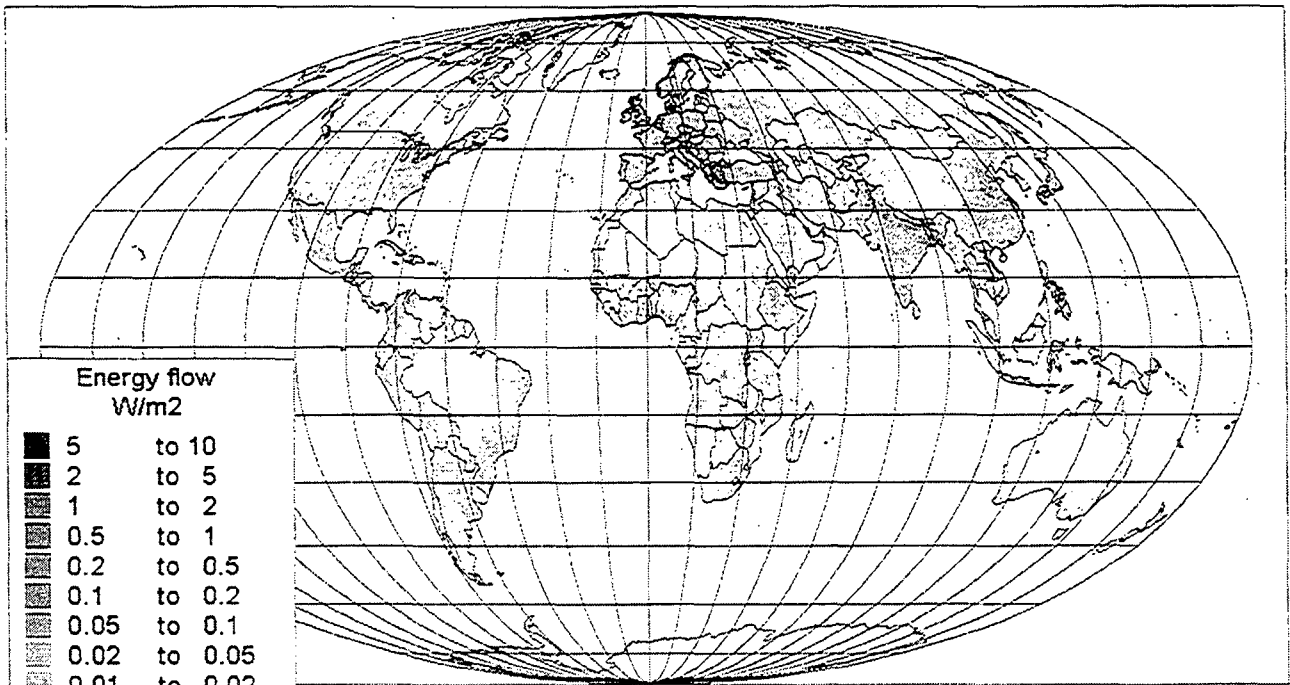
Energy flow W/m2		
5	to	10
2	to	5
1	to	2
0.5	to	1
0.2	to	0.5
0.1	to	0.2
0.05	to	0.1
0.02	to	0.05
0.01	to	0.02
0.005	to	0.01
0.002	to	0.005
0.0001	to	0.002
all others		

Energy flow
W/m2

5	to 10
2	to 5
1	to 2
0.5	to 1
0.2	to 0.5
0.1	to 0.2
0.05	to 0.1
0.02	to 0.05
0.01	to 0.02
0.005	to 0.01
0.002	to 0.005
0.0001	to 0.002
all others	

Figure 2c. July potential power production from building-integrated solar cells, with transmission and storage cycle losses subtracted (W/m^2, above). (based on [18]).
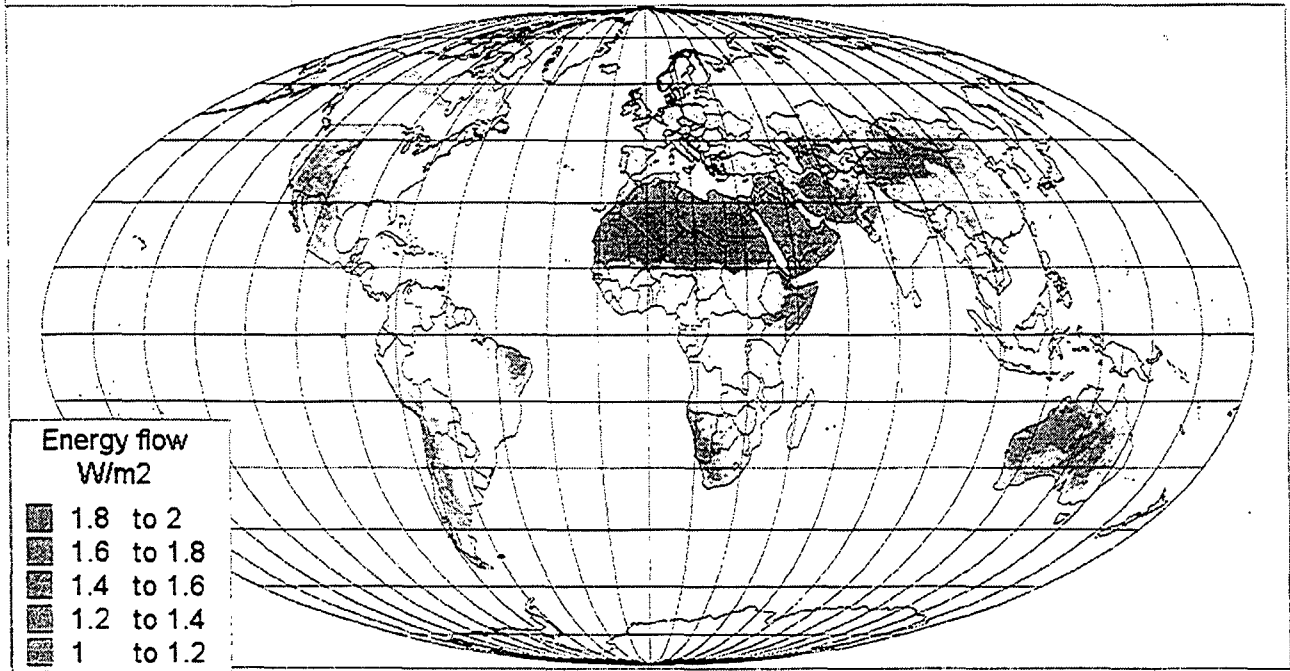
Energy flow
W/m2

1.8	to 2
1.6	to 1.8
1.4	to 1.6
1.2	to 1.4
1	to 1.2
0.8	to 1
0.6	to 0.8
0.4	to 0.6
0.2	to 0.4
0.01	to 0.2
all others	

Figure 3. Potential annual average power production from centralised photovoltaic plants on marginal land, with transmission and storage cycle losses subtracted. Seasonal variations are modest (W/m^2; scale is linear in contrast to that of Fig. 2). Based on [18].

61
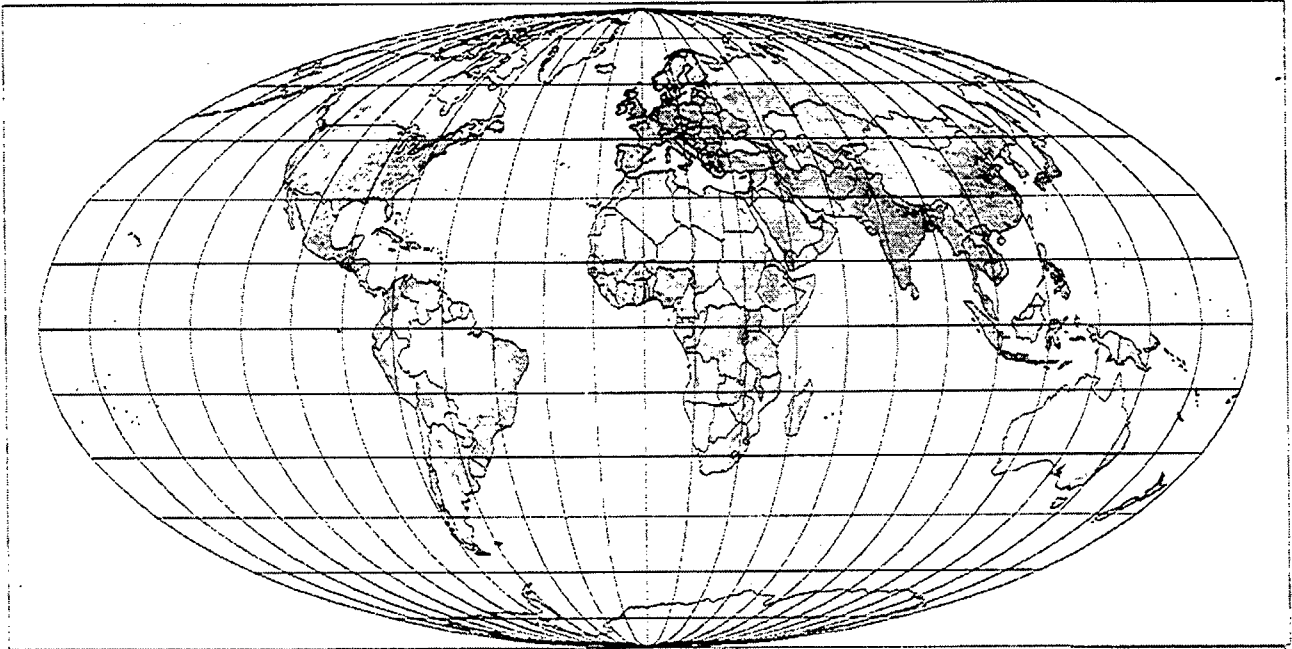
Figure 4. Total energy to be delivered to consumers in the 2050 scenario (including environmental heat, energy in food, and energy used for transportation and directly as electricity). The scale of average energy flow in watts per square metre of land area is given to the right (above; from [18]).
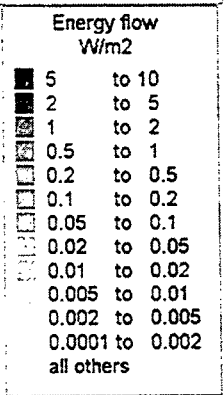
Figure 5 (below). Estimated total renewable energy resources, taking into account land restrictions due to alternative uses and environmental considerations, as well as conversion losses. The sources include solar photovoltaic, wind, hydro, all for producing electricity, and biomass used for fuels and food, given in units of energy flow (watts per square metre). From [18], where details of the individual resource estimates can also be found.
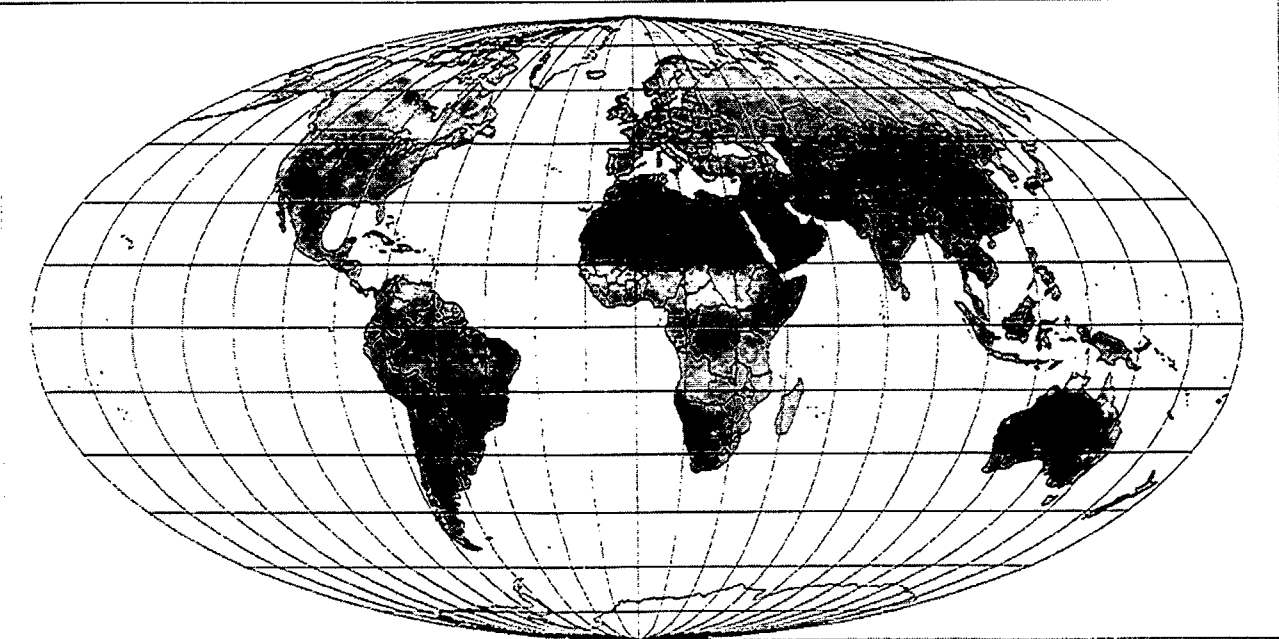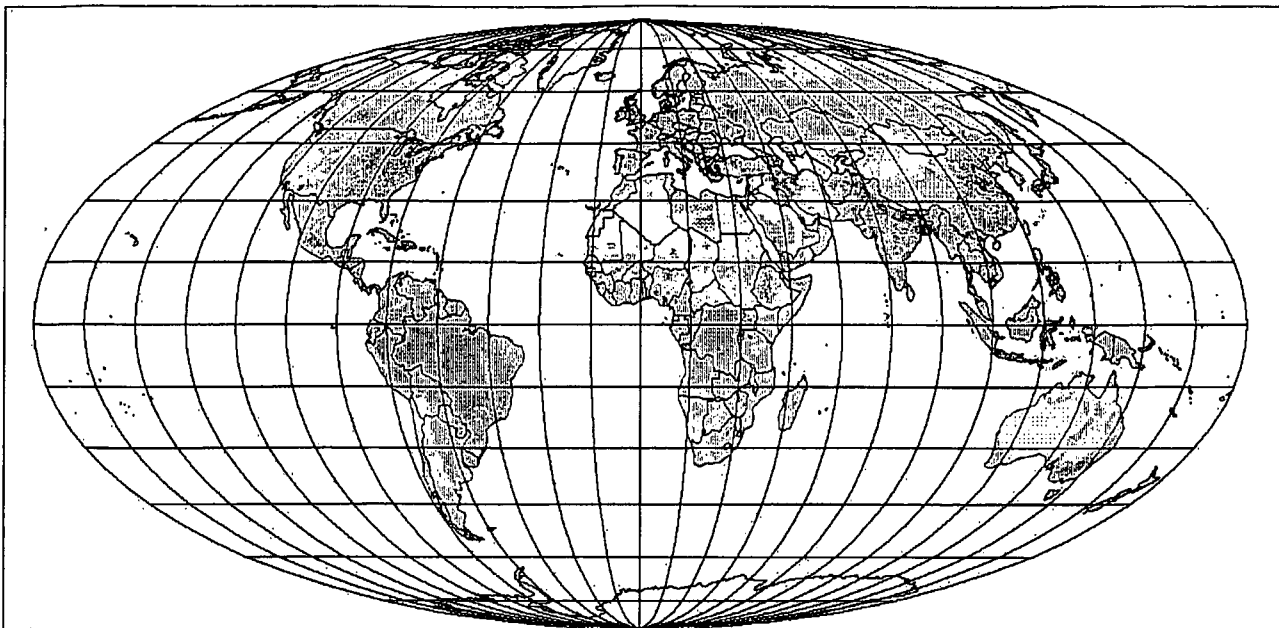
Energy flow W/m2		
5	to	10
2	to	5
1	to	2
0.5	to	1
0.2	to	0.5
0.1	to	0.2
0.05	to	0.1
0.02	to	0.05
0.01	to	0.02
0.005	to	0.01
0.002	to	0.005
0.0001	to	0.002
all others		

Figure 6 (above). Difference between supply and demand, for the decentralised renewable energy 2050 scenario, using only building-integrated solar cells and farm-attached wind turbines, together with pesticide-free agriculture and bio-energy production only from agricultural and forestry residues, plus existing hydro power. The delivered energy supply comprises food, electricity and biofuels for stationary and transportation uses. Unit W/m^2. From [18].

Figure 7 (below). Difference between supply and demand, for the centralised renewable energy 2050 scenario, using building-integrated and centralised solar cells on marginal land, wind turbines near farms and in parks on marginal land or off-shore, together with pesticide-free agriculture and bio-energy production from residues and a limited number of energy-crops or energy-forests, plus hydro power in place or under construction. The delivered energy supply comprises food, electricity and biofuels for stationary and transportation uses. Unit W/m^2. From [18].

Figure 8. Overview of centralised 2050 renewable energy scenario (energy flows in GW or GWy/y). From [18].